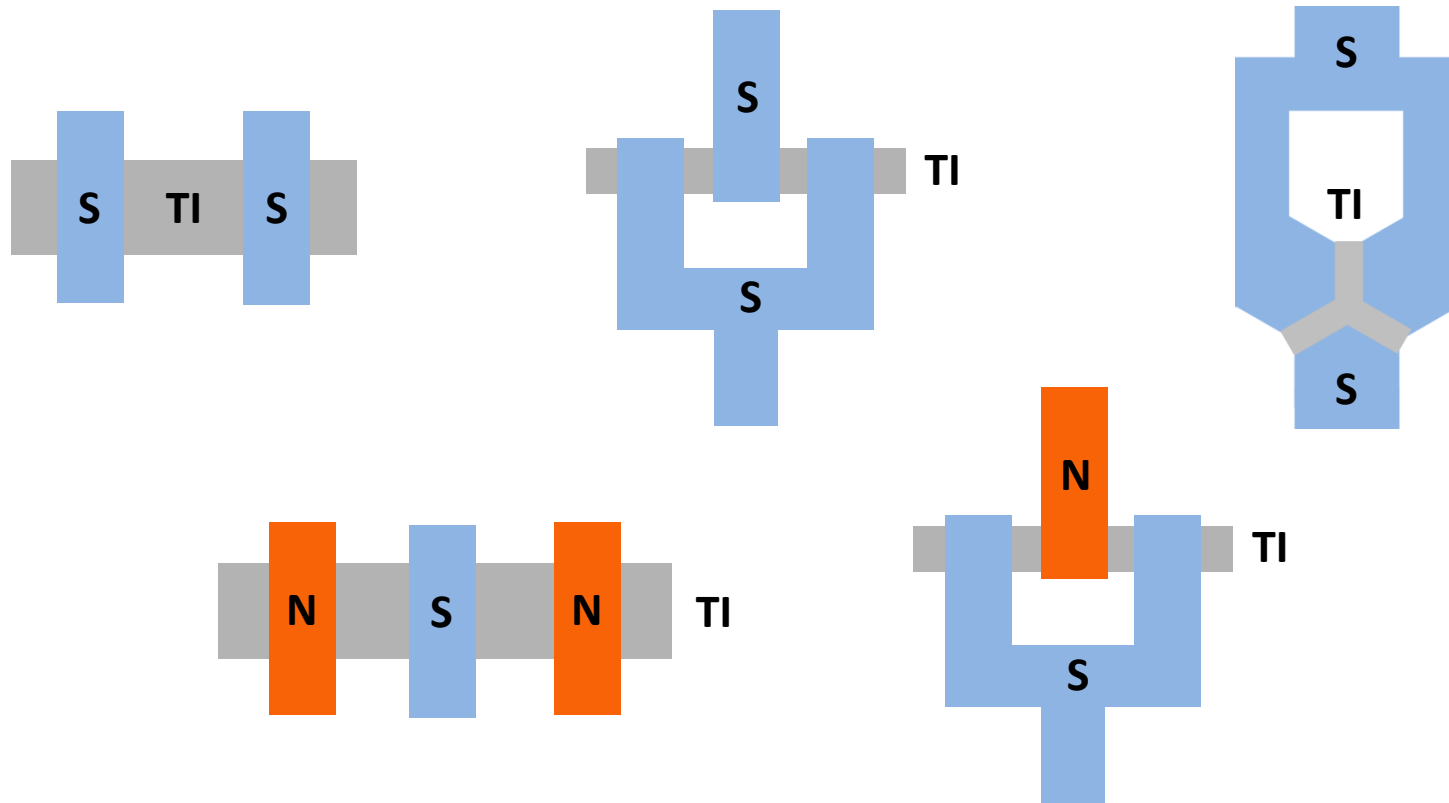


“Phase Coherence and Josephson phenomena in hybrid superconductor-topological insulator devices”



Dale J. Van Harlingen

University of Illinois at Urbana-Champaign

UIUC research team and collaborators

Experiments

Aaron Finck

POSTDOC UIUC



IBM Yorktown Hts.

Cihan Kurter

POSTDOC UIUC



MISSOURI S&T

Erik Huemiller

GRAD UIUC



Can Zhang

GRAD UIUC



Vlad Orlyanchik

POSTDOC UIUC



*Accio Energy
Ann Arbor, MI*

Martin Stehno

POSTDOC UIUC



*University of Twente
Netherlands*

Samples

Seongshik Oh

RUTGERS



MBE Ti films

Yew San Hor

MISSOURI S&T



Ti crystals

Pouyan Ghaemi

POSTDOC ILLINOIS



CCNY

**Smitha
Vishveshwara**

UIUC



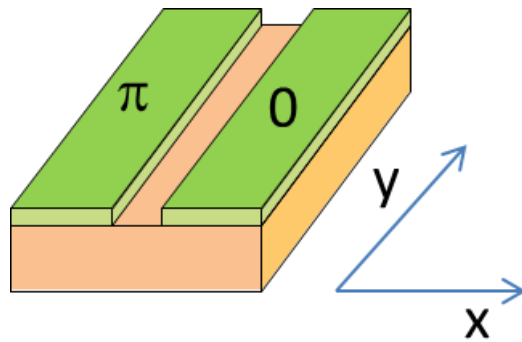
Taylor Hughes

UIUC



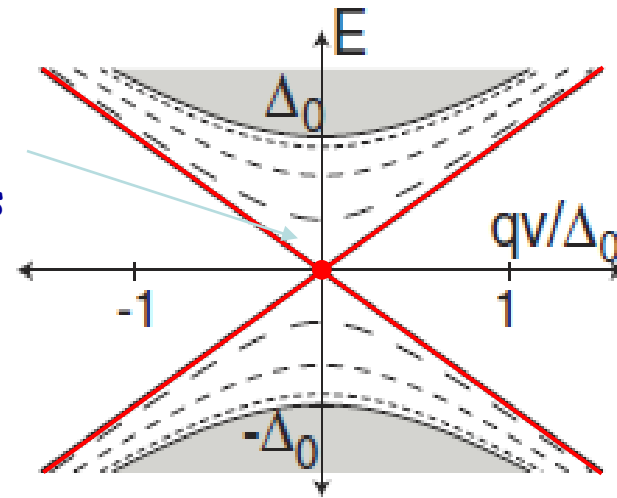
Andreev Bound States (ABSs) in S-TI-S Josephson junctions

L. Fu and C. Kane, Phys. Rev. Lett. 100, 096407 (2008)



$L \rightarrow 0$

Zero energy
Majorana
Bound states



ABS energy levels

$$E_{\pm}(q, \phi) = \pm \sqrt{v^2 q^2 + \Delta^2 \cos^2(\phi/2)}$$

$$E_{\pm}(\phi) = \pm \Delta \cos(\phi/2) \quad \text{for } q=0$$

Supercurrent
contribution

$$I_{\pm}(\phi) = \frac{2e}{\hbar} \frac{\partial E_{\pm}}{\partial \phi} = \mp \left(\frac{e\Delta_0}{2\hbar} \right) \frac{\sin \phi}{\sqrt{\frac{v^2 q^2}{\Delta_0^2} + \cos^2\left(\frac{\phi}{2}\right)}}$$

Low-energy ABS:

$$I \propto \sin \phi$$

for q small

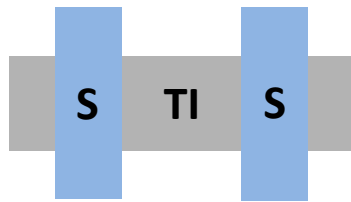
(skewed CPR)

Majorana states:

$$I \propto \sin \frac{\phi}{2}$$

for $q=0$

(4π -periodic CPR)



Why lateral S-TI-S junctions?

Not the favorite system of most because of the complexity:

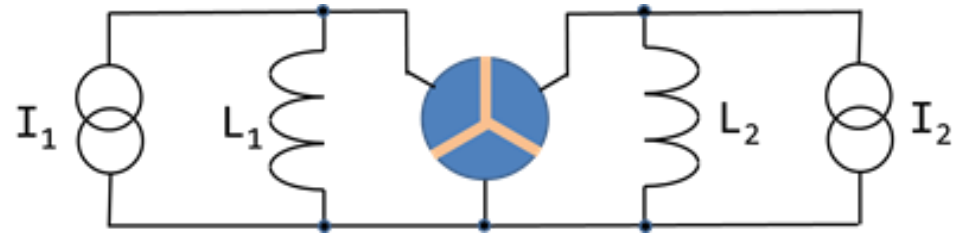
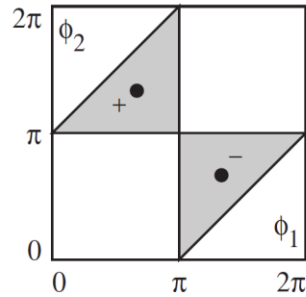
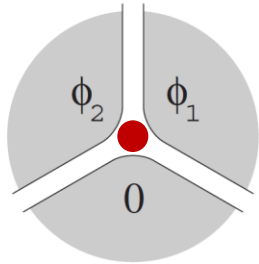
- 2D width (multiple channels)
- Multiple surfaces (top, edges, bottom)
- Conducting bulk states and trivial surface states in the TI

Advantages:

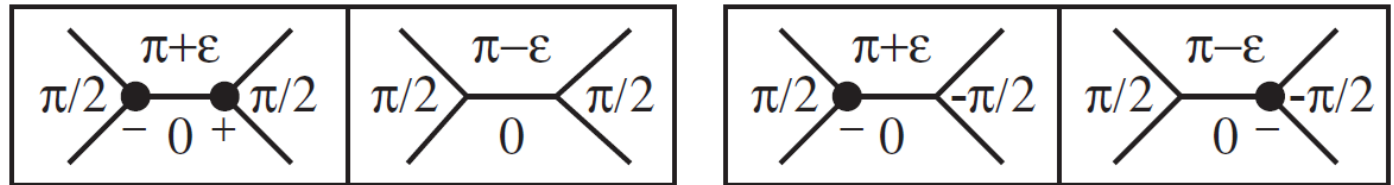
- Supports topological excitations without a strong magnetic field. Allows use of phase-sensitive techniques.
- Access to barrier. Allows probes and imaging.
- Expandable into networks.
- Several modes of operation to move and control Majorana fermions by phase, current, or voltage.
- Schemes proposed to braid and perform logical operations.

Phase-controlled devices

Lateral junctions circuits --- Majorana fermions nucleated at trijunctions

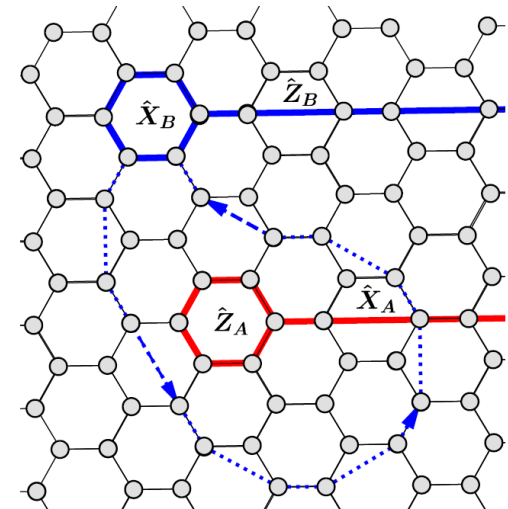
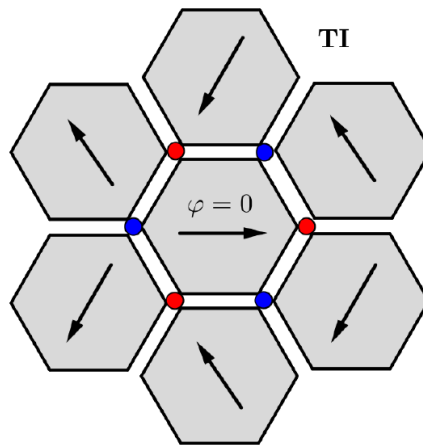


Fu and Kane



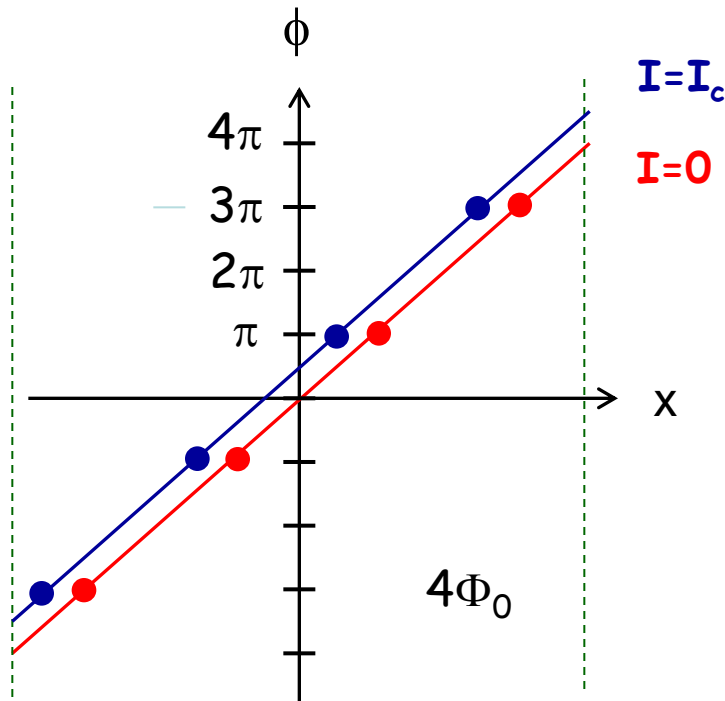
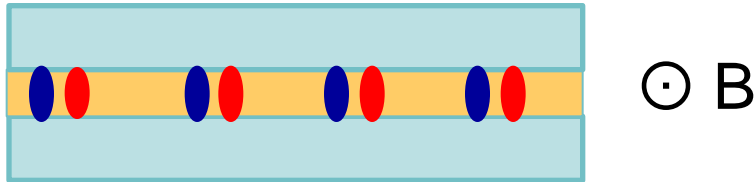
Majorana fermion
surface code
scheme

Vijay, Hsieh, and Fu



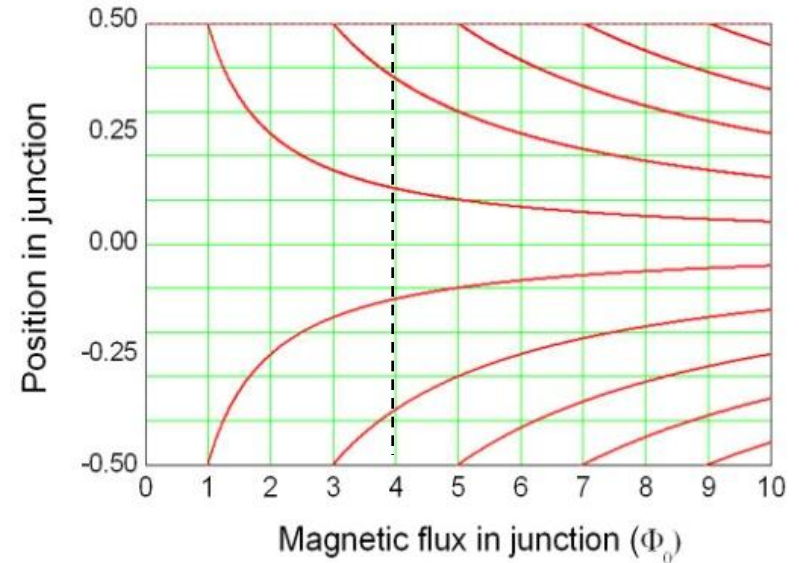
Current-controlled devices: lateral junctions in a magnetic field

Perpendicular magnetic field induces a phase gradient across the junction

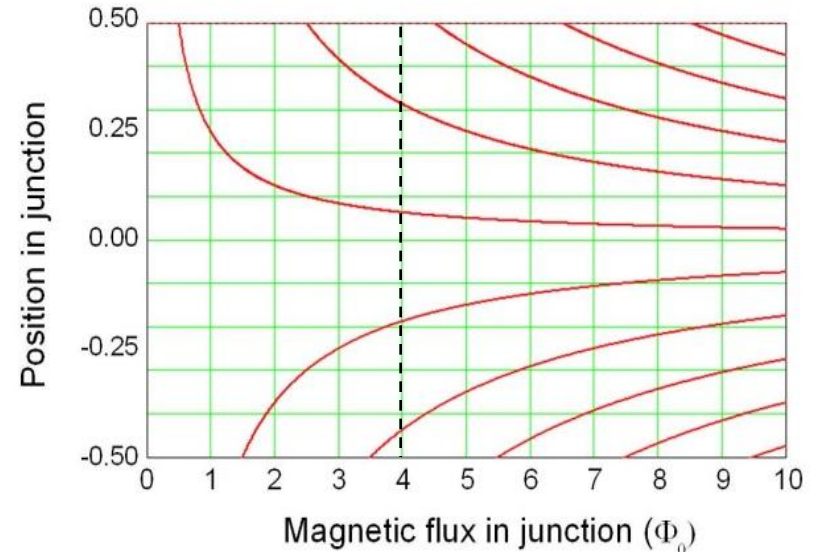


Majorana fermions enter junction attached to Josephson vortices --- located where the phase difference is an odd multiple of π

Zero current: MFs enter symmetrically



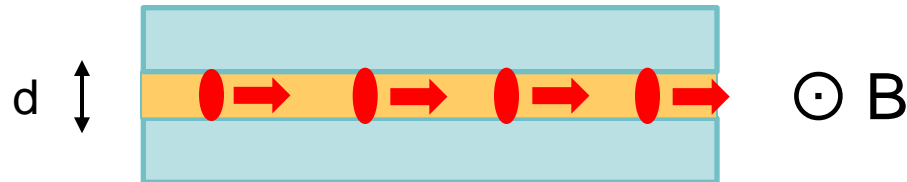
At critical current: MFs enter alternatively



Voltage-controlled devices: moving Majorana fermions

Phase winds according to the Josephson relation: $\frac{d\phi}{dt} = \frac{2eV}{\hbar}$

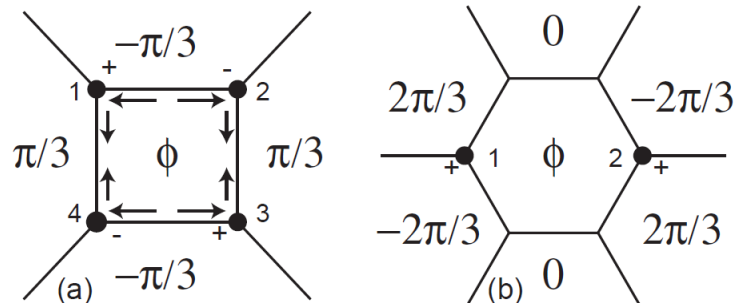
Majorana fermions move laterally through junction at speed: $v = \frac{V}{Bd}$



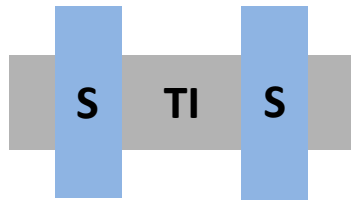
For $V = 1 \mu\text{V}$ and $d = 100 \text{ nm}$ and $B = 10 \text{ mT}$, $v = 1 \text{ km/s}$!

Provides way to move Majorana fermions fast along lateral junctions

Could be used to manipulate MFs in multiply-connected junction networks for braiding:



Fu and Kane



Agenda

Transport in Nb-Bi₂Se₃-Nb junctions

- Long-range phase coherence of topological surface states
- Phase transition in the location of the topological surface state

Josephson interferometry in Nb-Bi₂Se₃-Nb junctions and SQUIDS

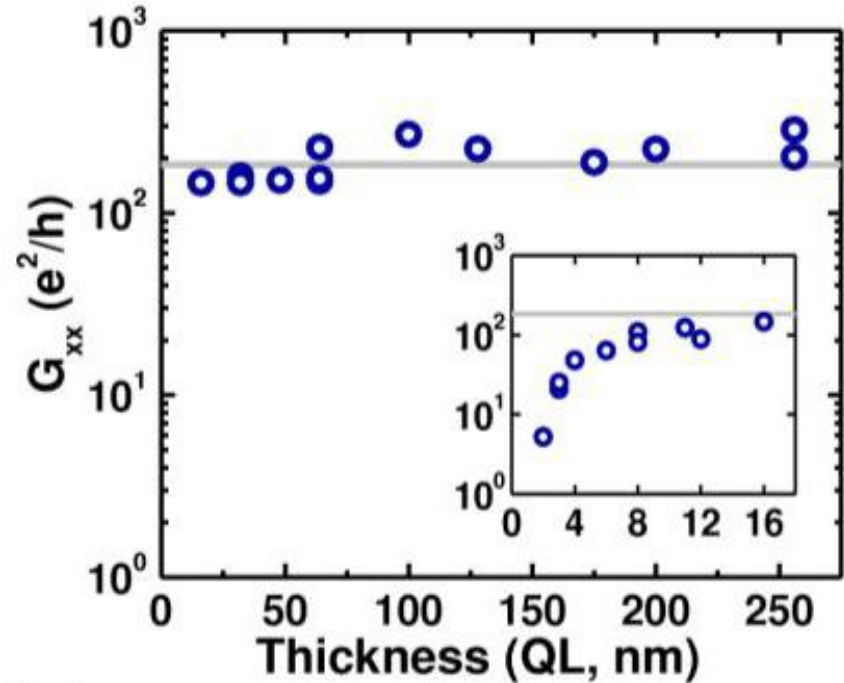
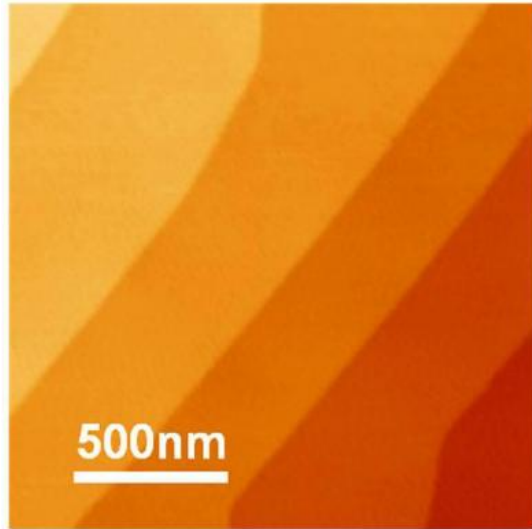
- Node-lifting of the magnetic field modulation patterns
- Non-sinusoidal components in the current-phase relation
- Evidence for 4π -periodicity that could arise from Majorana states

Interference experiments in hybrid Nb-Bi₂Se₃ structures

- Order parameter of proximity-induced superconductivity
- Conductance channels induced by superconductor dots
- Aharonov-Casher experiment in lateral junctions

Bi₂Se₃ Materials Characteristics

- Bi₂Se₃ film MBE-grown on Al₂O₃



Bulk is insulating - conductance is dominated by **two surface channels**:

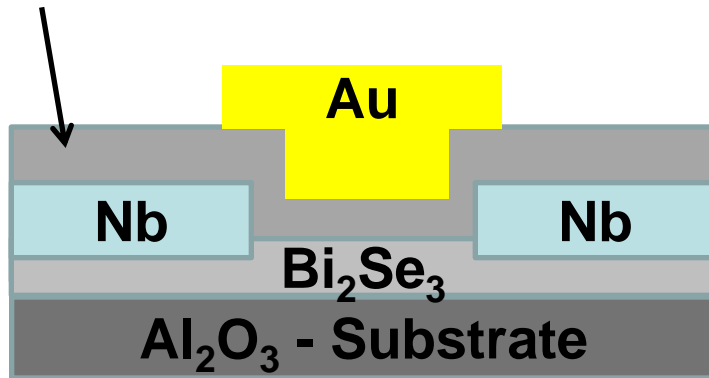
1. Trivial 2DEG (2-3 quintuple layers)
2. Topological surface state

- Bi₂Se₃ exfoliated crystals

Bulk is generally more conducting but we expect the surface state properties to be similar

Nb/Bi₂Se₃/Nb Josephson Junctions

Gate Dielectric ALD Al₂O₃/HfO₂



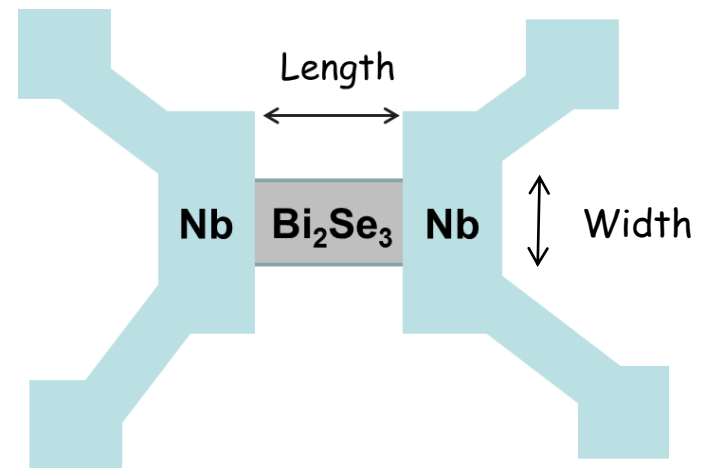
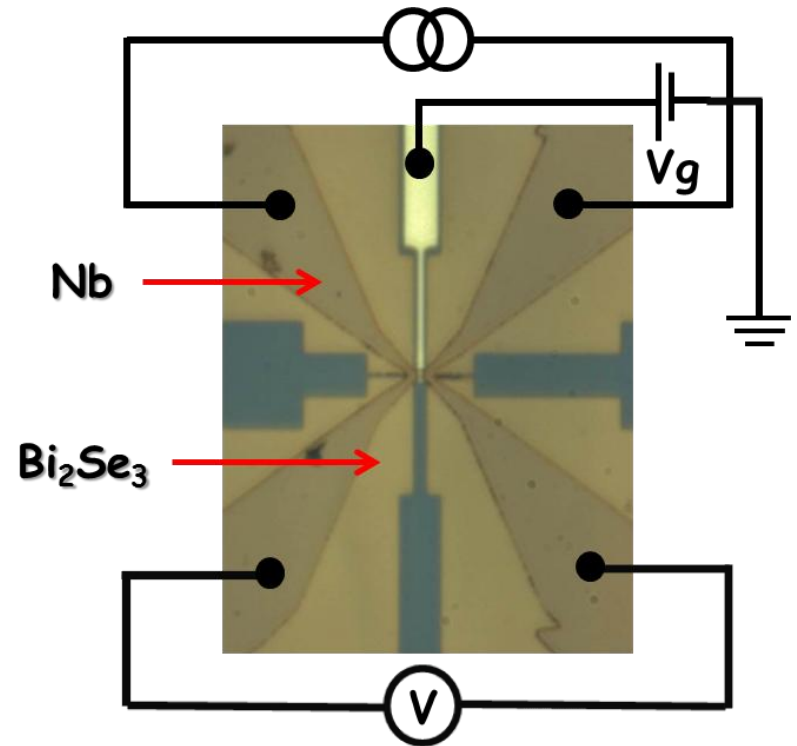
- E-beam lithography
- Ion milling
- Evaporation and sputtering

Typical Dimensions:

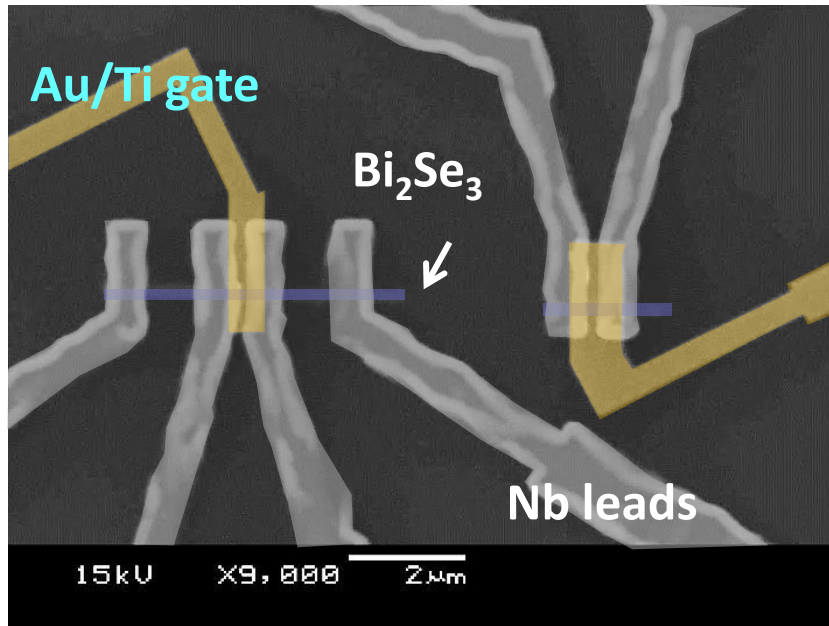
Length = 100-300nm

Width = 300nm-1μm

Top gate dielectric ~ 35-40nm
(ALD Al₂O₃/HfO₂)



Nb/Bi₂Se₃/Nb Josephson Junctions on Exfoliated Crystals

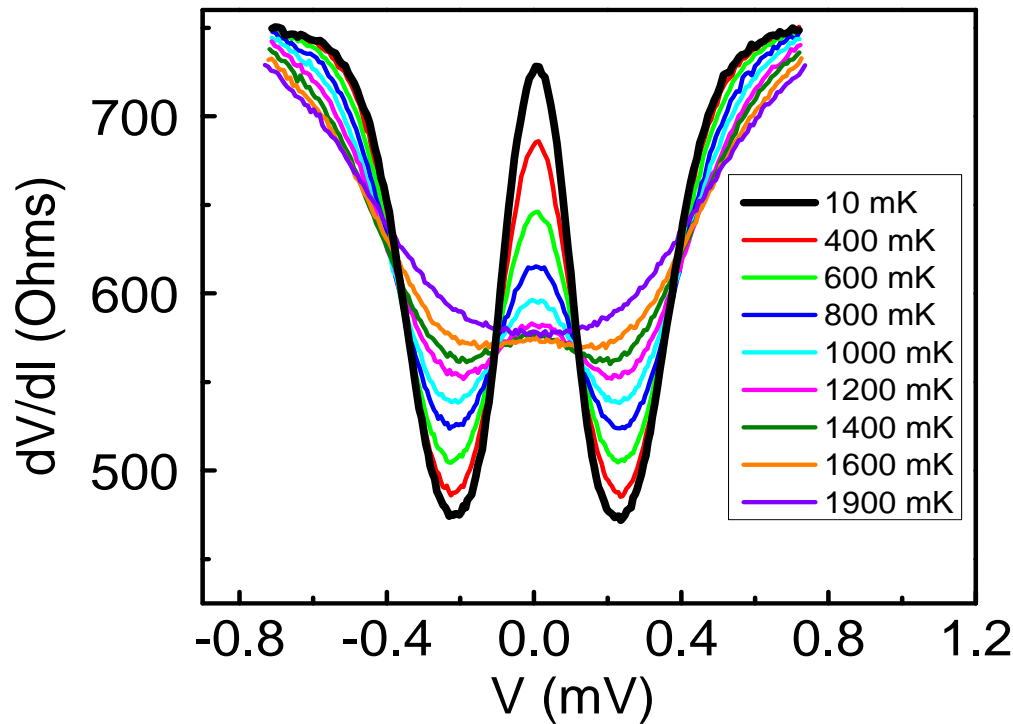
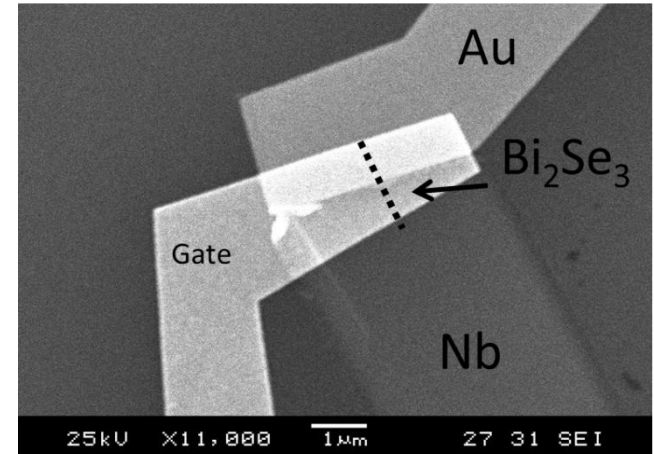
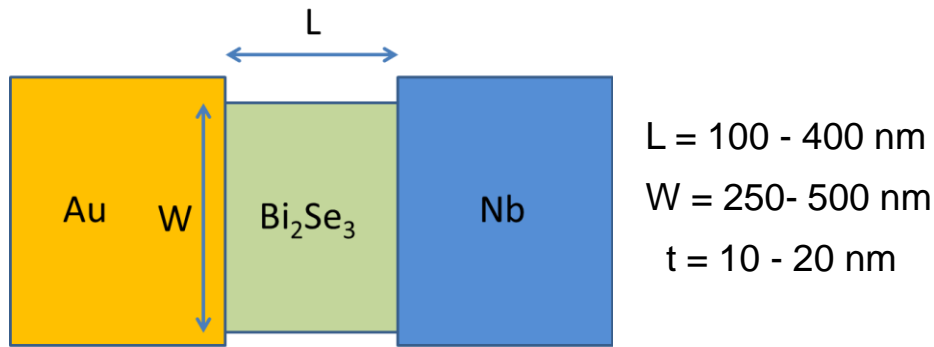


We see the same behavior in thin film and exfoliated crystals of all thicknesses, independent of the relative width of the SC and TI:

This suggests that:

1. Most of the supercurrent is carried by the top surface.
2. Bulk conductance does not play a large role in the supercurrent properties.

Transport in Nb-Bi₂Se₃-Cu structures



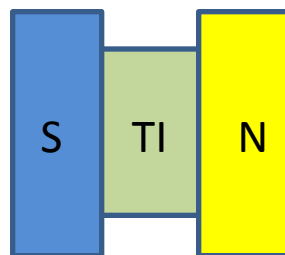
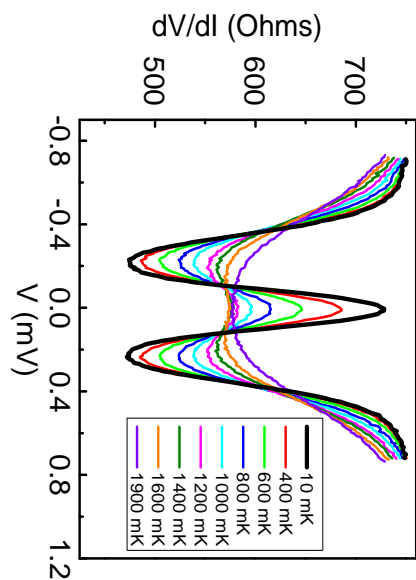
Re-entrant resistance: competition between quasiparticle diffusion and the proximity-induced energy gap

$$E_T = \frac{\hbar D}{L^2},$$

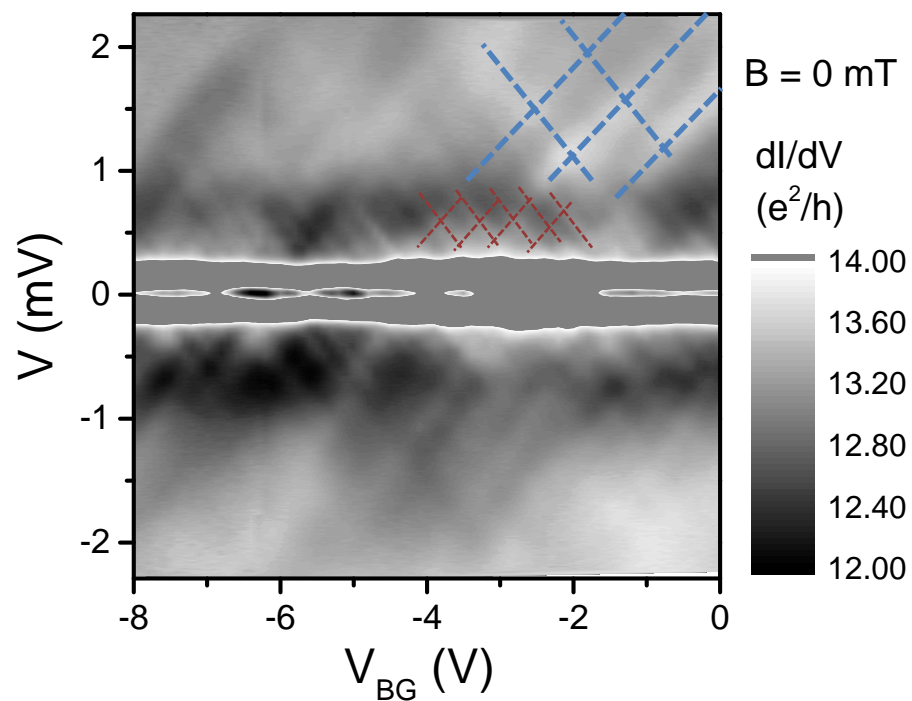
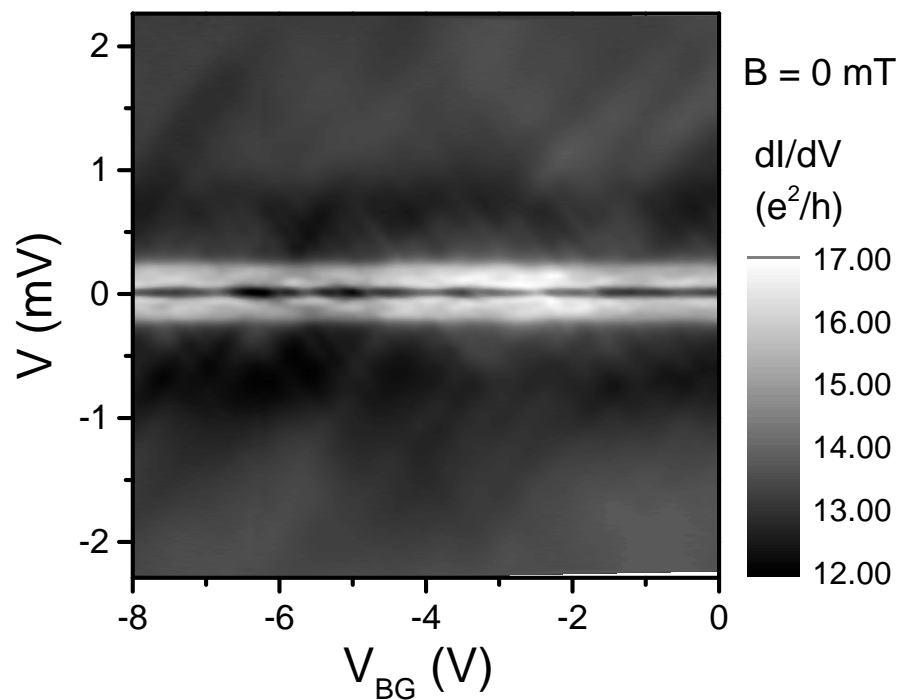
$$D = \frac{1}{2} v_F l \approx 0.0025 \text{ m}^2 / \text{s}$$

For $L = 100 \text{ nm}$: $E_T = 160 \text{ mV}$

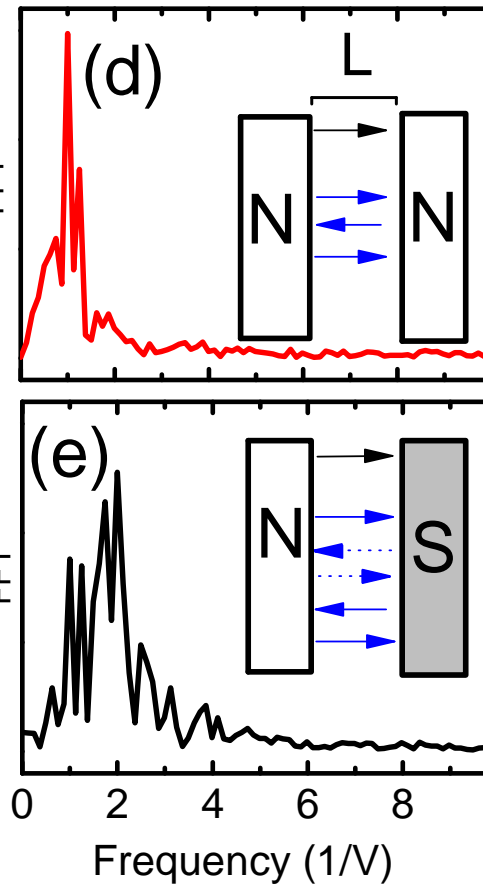
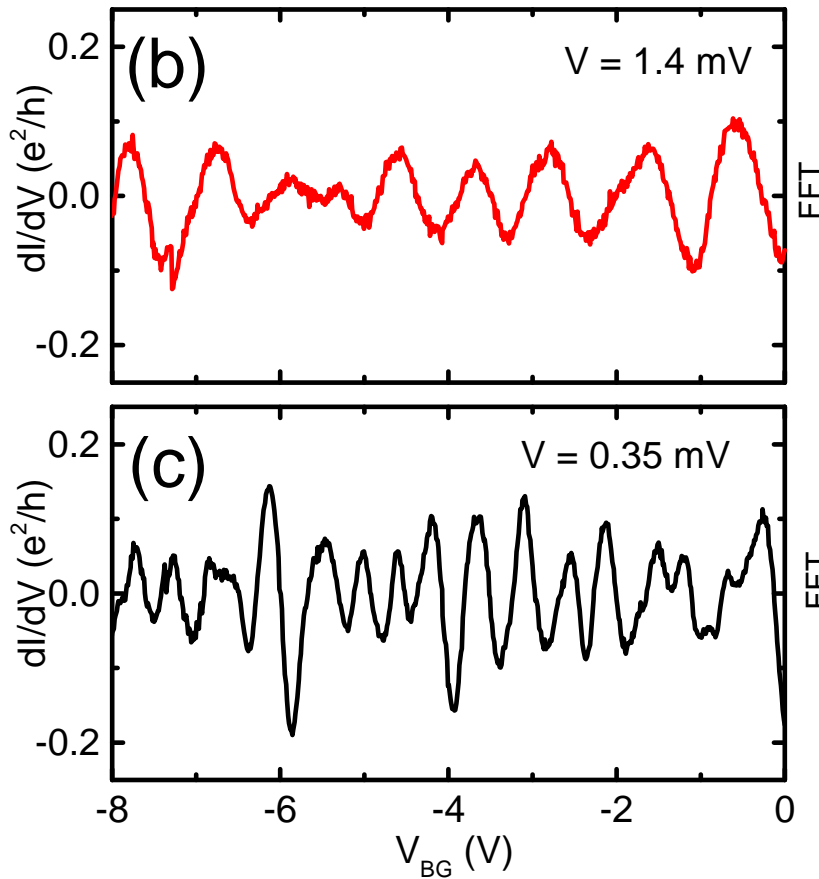
Gate-Tuned Transport



9 nm thick TI flake
 $L = 230$ nm



Fabry-Perot and Andreev Oscillations



Fabry-Perot

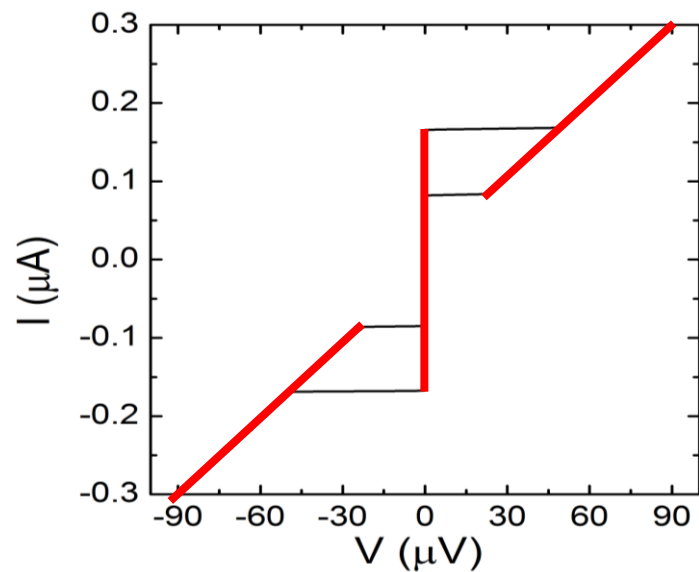
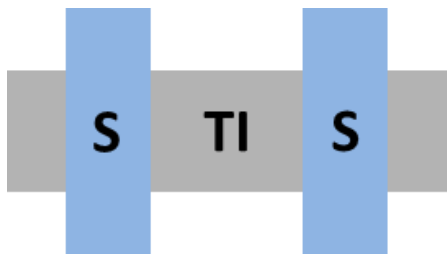
$$DE_F = \frac{h v_F}{2L}$$

Andreev

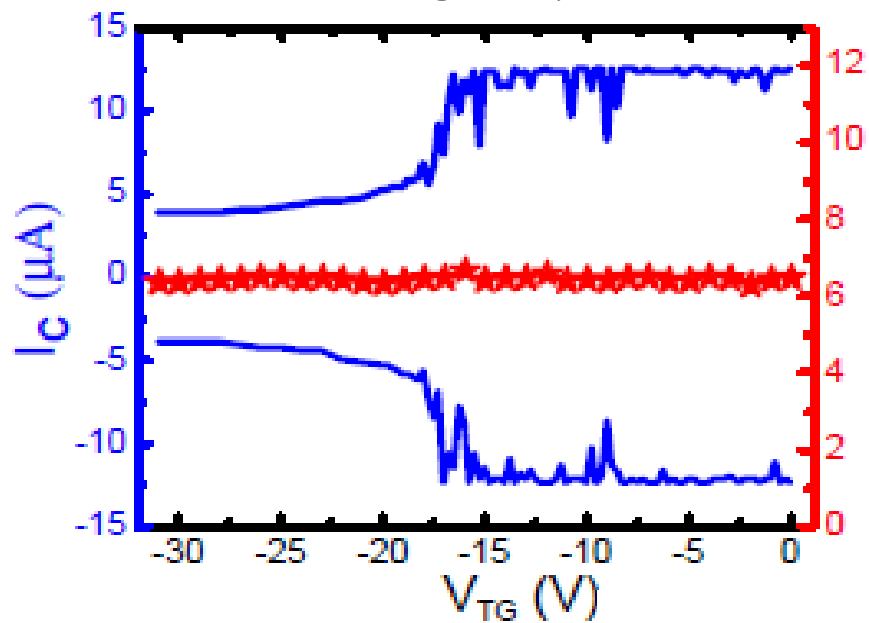
$$DE_F = \frac{h v_F}{4L}$$

**Josephson Interferometry
in Nb-Bi₂Se₃-Nb junctions**

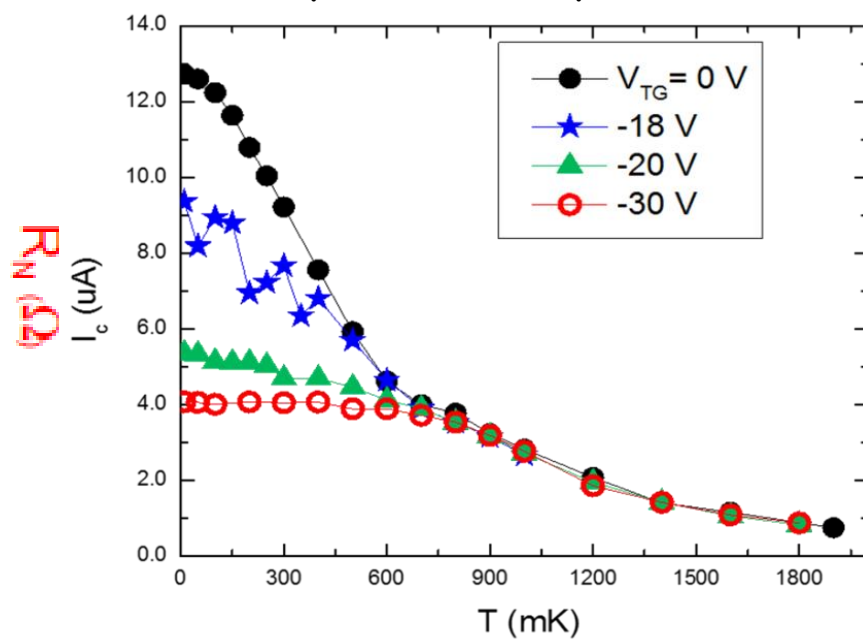
Supercurrents



Gate voltage dependence



Temperature dependence

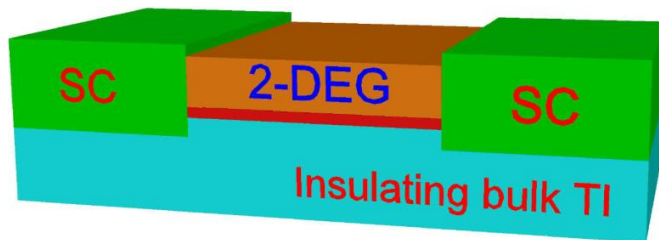


Gate dependence model (Pouyan Ghaemi)

Shift in the location of the topological surface state from below to above the trivial 2-DEG surface states as gate voltage depletes them

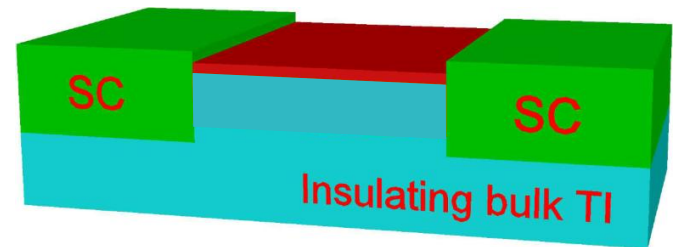
Low gate voltage:

- Fermi energy in conductance band
- Topological surface state buried

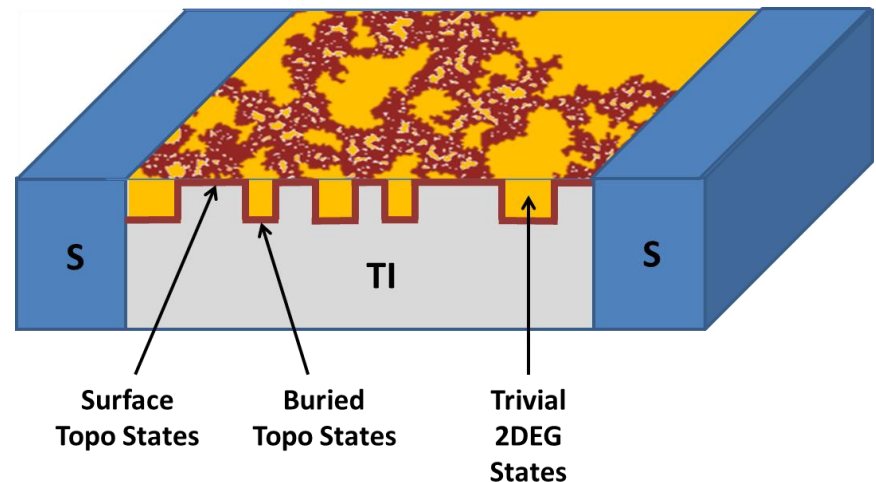


High (negative) voltage:

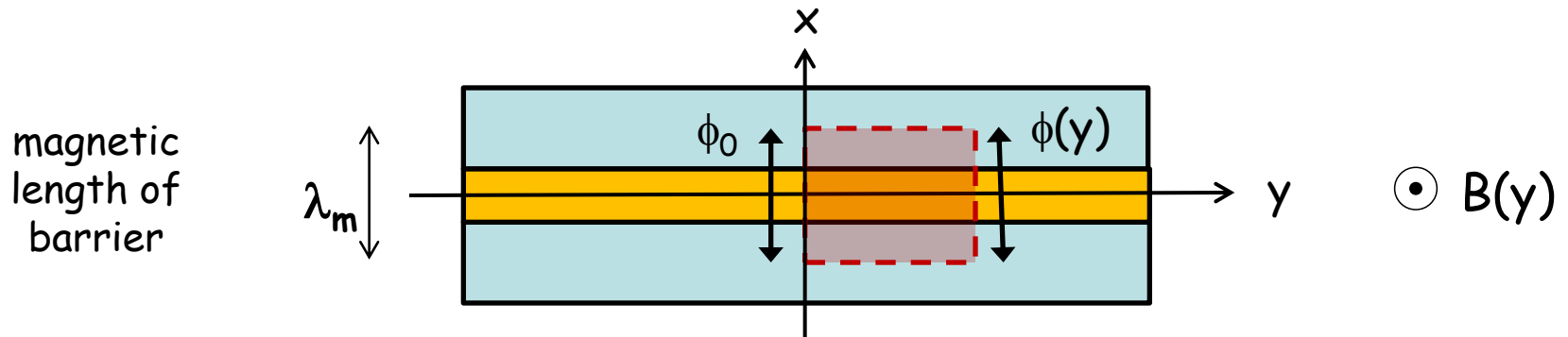
- Fermi energy in the band gap
- Topological surface state on surface



Near crossover, spatial charge fluctuations create a dynamically-meandering topological surface state



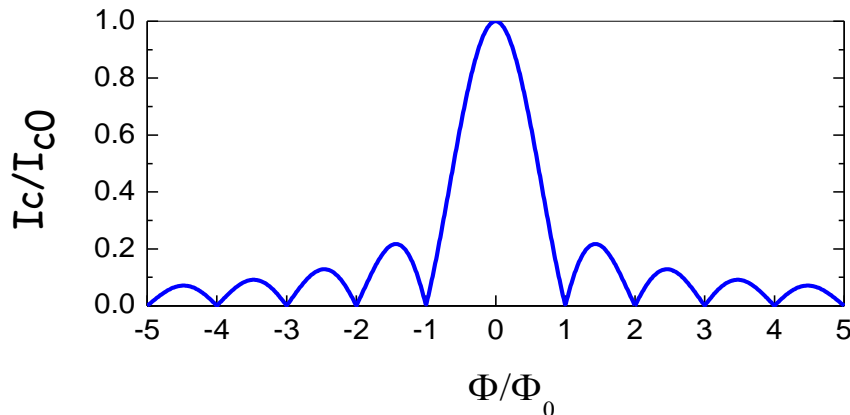
Josephson Interferometry: response to a magnetic field



Magnetic field induces a phase variation: $\phi(y) = \phi_0 + \frac{2\pi}{\Phi_0} \int_0^y dy' \lambda_m B(y')$

Uniform field $\Rightarrow \phi(y) = \phi_0 + \frac{2\pi}{\Phi_0} \lambda_m B y \Rightarrow$ *linear phase variation*

$$I_c = \max \int_{-w/2}^{w/2} dy t J_c \sin(\phi_0 + \frac{2\pi}{\Phi_0} \lambda_m B y)$$



Fraunhofer diffraction pattern

Josephson Interferometry: what it can tell you about

$$I_c(\Phi) = \max \int_{-w/2}^{w/2} dy t J_c(y) \text{cpr} \left(\phi_0 + \phi_{op}(y) + \frac{2\pi}{\Phi_0} \left(\Phi + \int_0^y dy' d_m \delta B(y') \right) \right)$$

**Critical
current
variation**

Gap anisotropy
Domains
Charge traps

**Current-
phase
relation**

Non-sinusoidal processes
 π -junctions
Exotic excitations
e.g. Majorana fermions

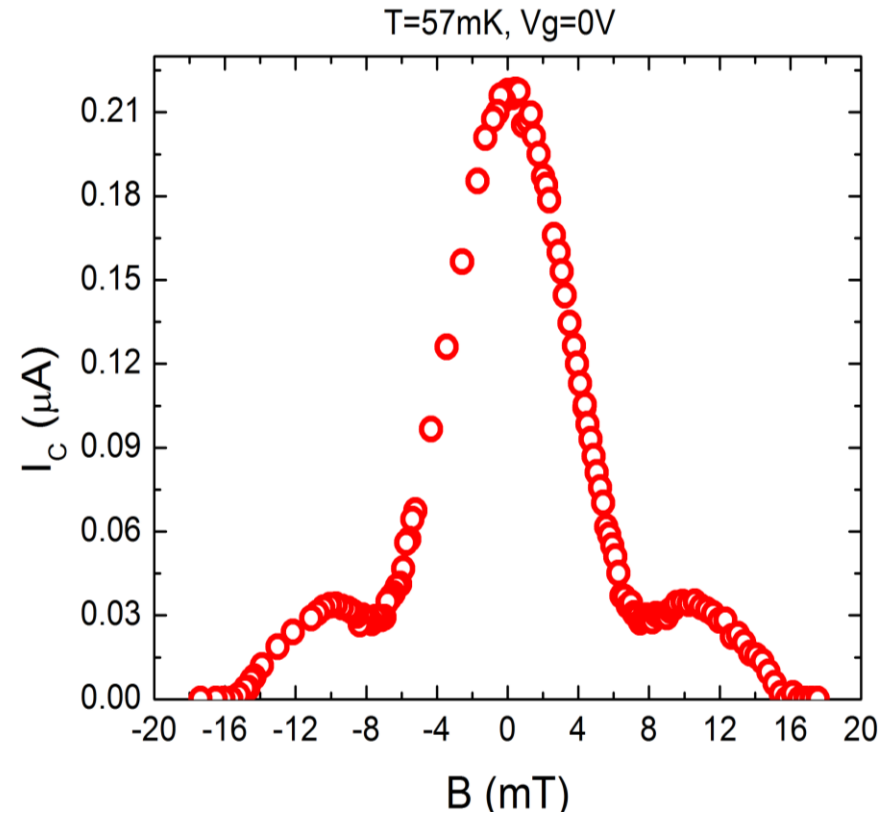
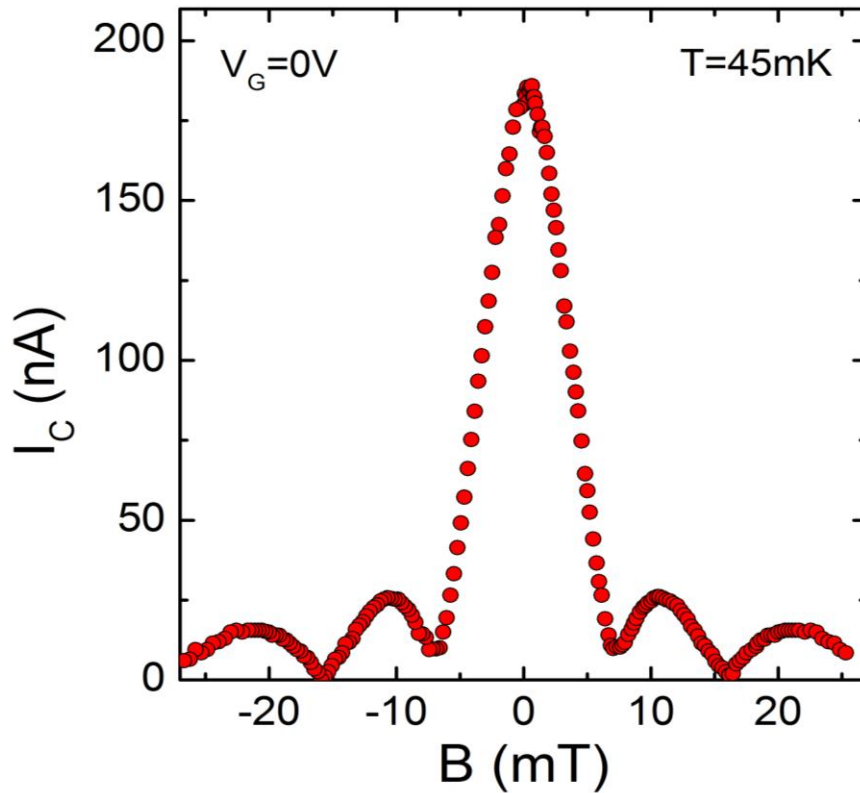
**Order
parameter
symmetry**

*Unconventional
superconductivity*

**Magnetic
field
variations**

Flux focusing
Trapped vortices
Magnetic particles

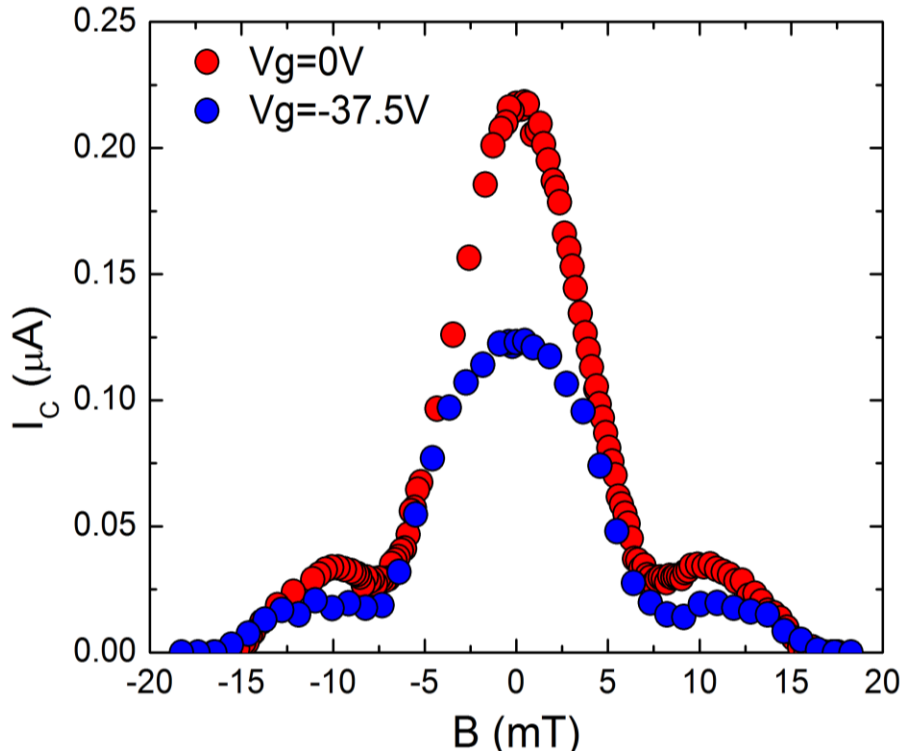
Supercurrent diffraction patterns



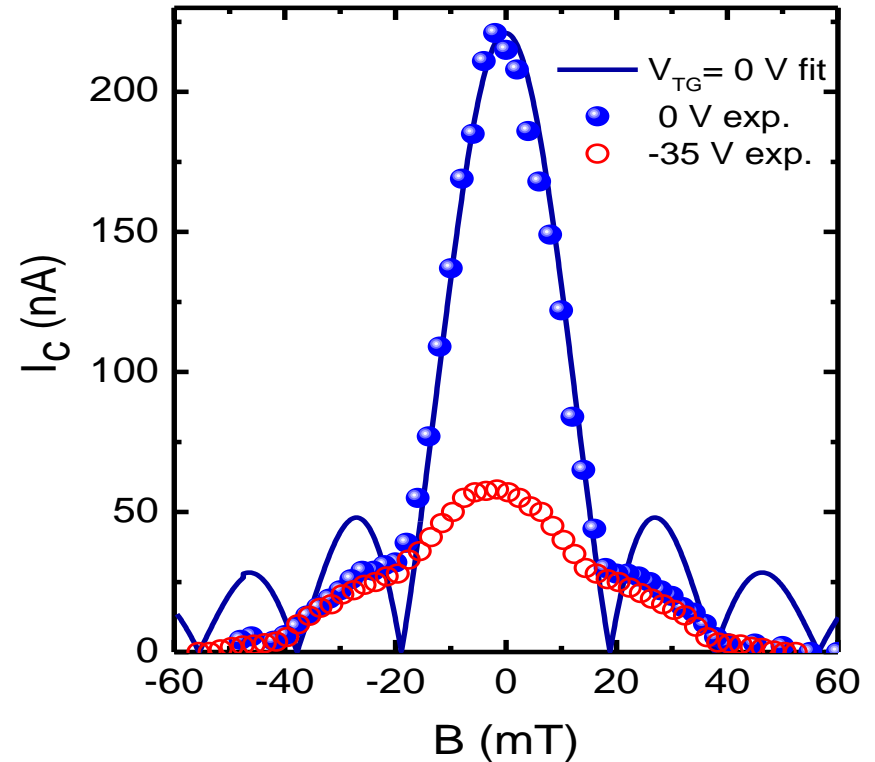
- 1st minimum does not go to zero
- 2nd minimum does go to zero

Diffraction pattern vs. gating

MBE-grown barrier

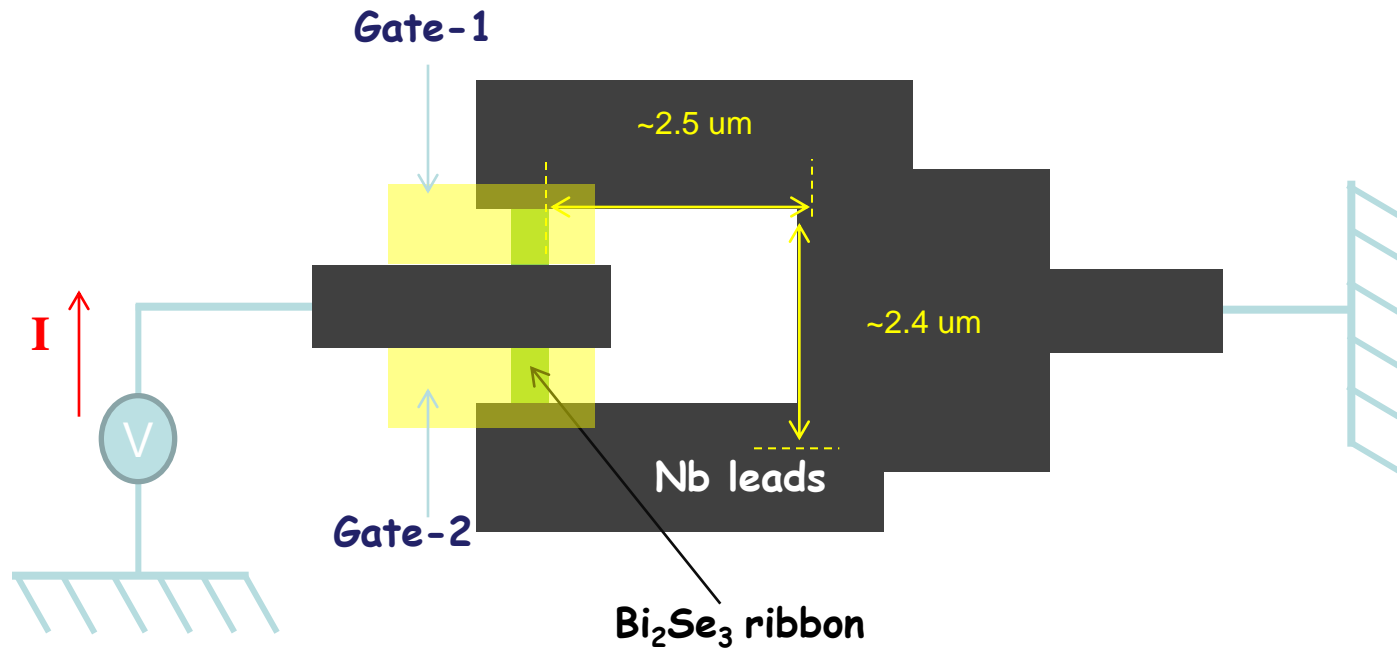


exfoliated barrier



- Central peak drops at Dirac point
- Side lobe is nearly unchanged
- Lifting of first node robust

dc SQUID w/ Nb-Bi₂Se₃-Nb



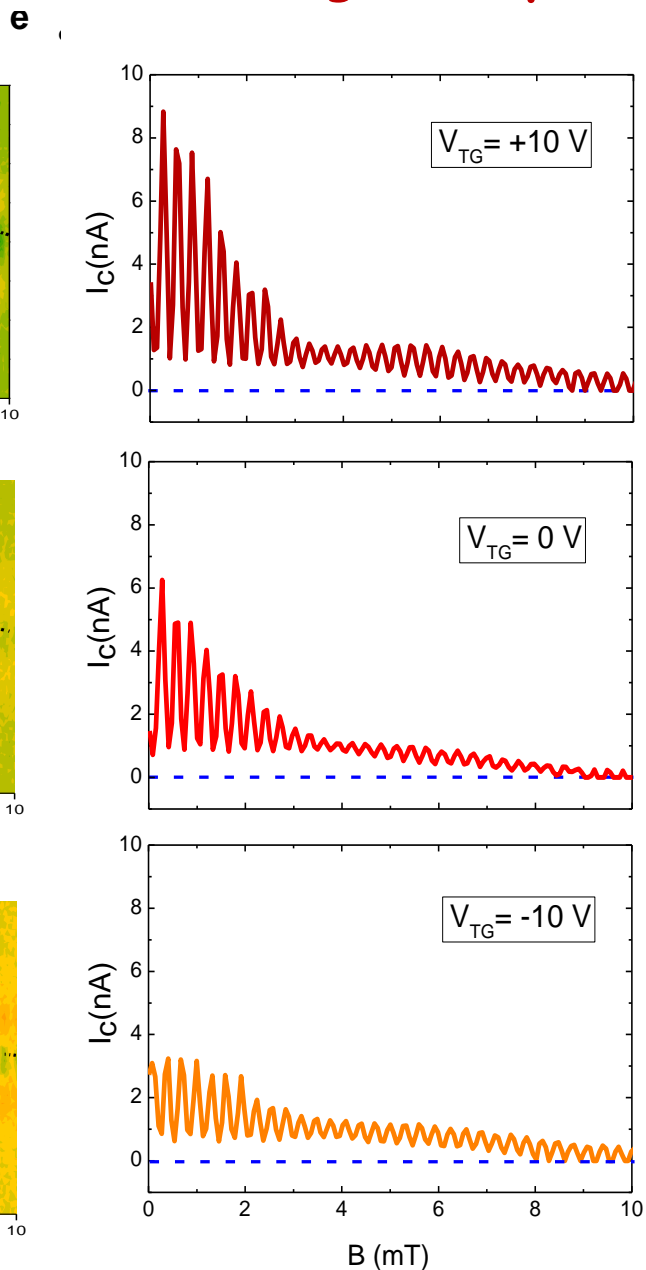
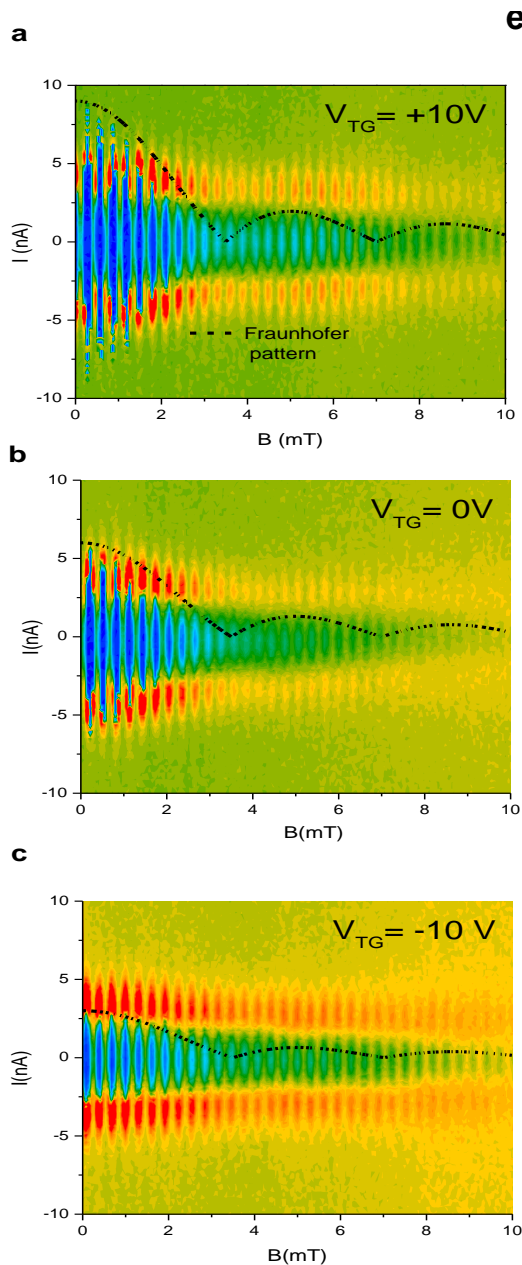
Bi₂Se₃: 19 nm thick , 4 μm long, 300 nm wide exfoliated piece
Junctions: length 300 nm, width 300 nm

Area loop ~ 6 μm²

Area junction ~ 0.9 μm²

} ratio ~ 60

SQUID oscillations --- gate dependence --- envelopes

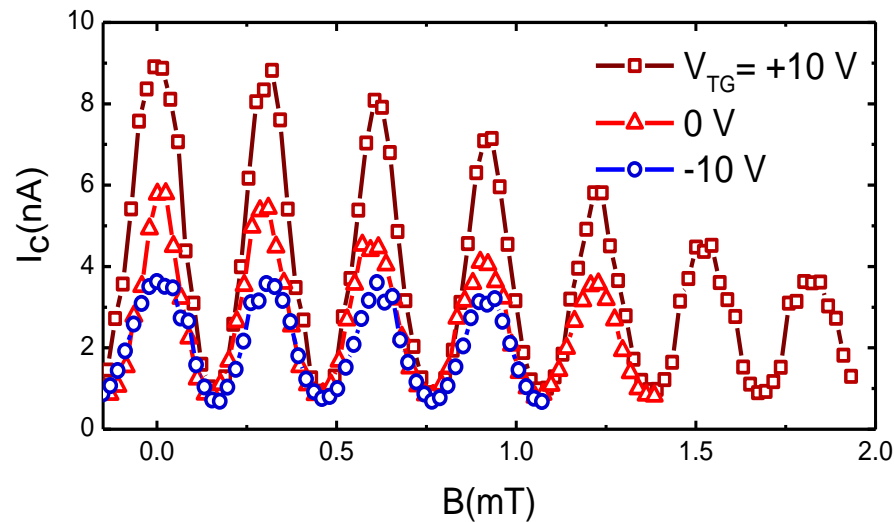
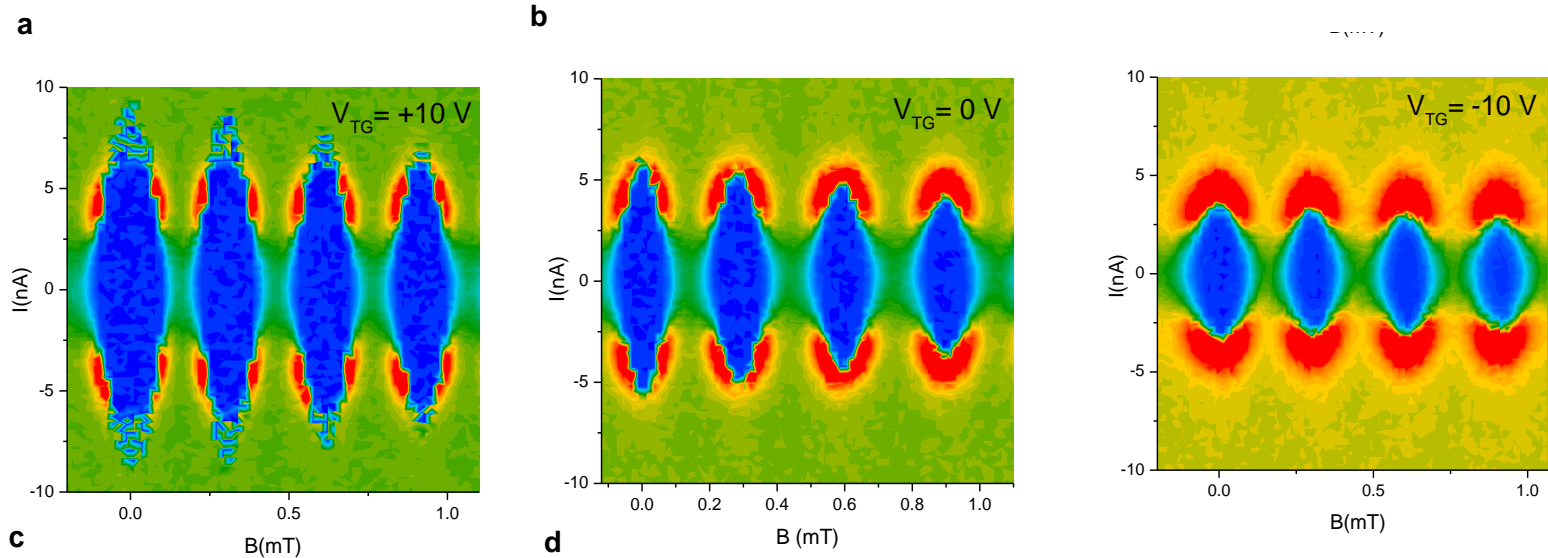


Envelopes exhibit same behavior as single junction diffraction: first node stays high, second vanishes

SQUID oscillations also do not go to zero as would be expected for $\beta \ll 1$ and a symmetric SQUID

$$\beta = 2\pi L I_c / \Phi_0$$

SQUID oscillations --- gate dependence



Modulation depth is gate-dependent: peaks drop; nodes stay constant

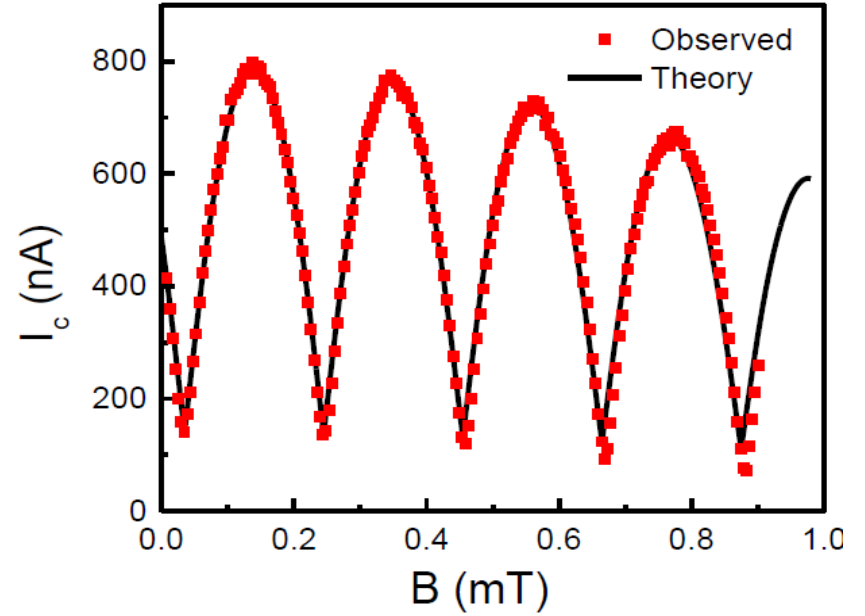
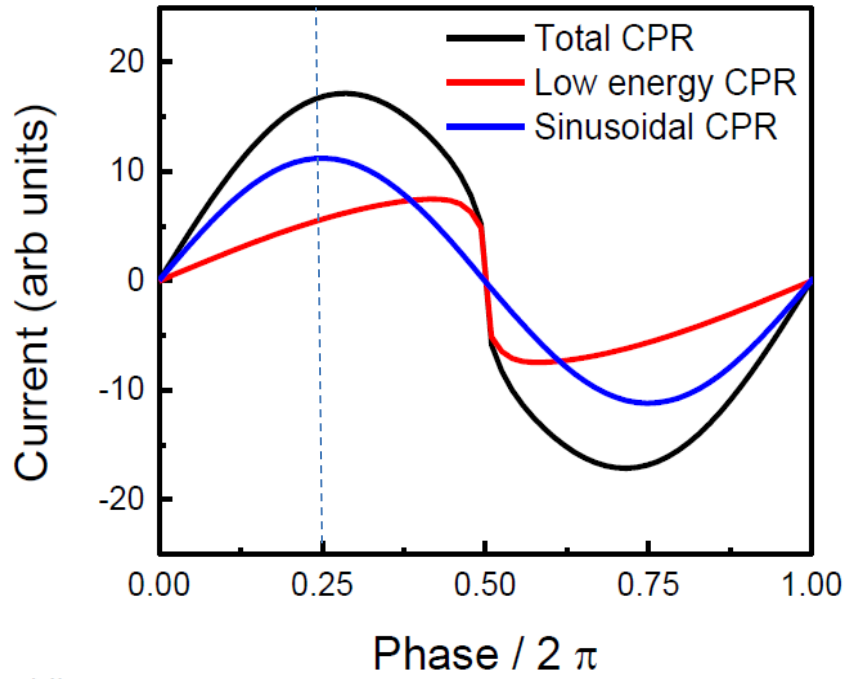
Node-lifting in dc SQUIDs

dc SQUIDs:

- Finite inductance of SQUID loop $\beta = 2\pi LI_c / \Phi_0$
Too small $\beta \ll 1$ ($\sim 10^{-3} - 10^{-4}$)
- Asymmetry in the junction critical currents $\alpha = (I_{c1} - I_{c2}) / (I_{c1} + I_{c2})$
Too small $\alpha < 0.1$ ($\sim 0.01 - 0.05$)
- Asymmetry in the SQUID loop inductance $\eta = (L_1 - L_2) / (L_1 + L_2)$
Too small $\eta \ll 0.1$ (~ 0.01)
- Skewness in the current-phase relation $s = (2\phi_{\max} / \pi) - 1$
Possible! SQUID node requires $I(\phi) = -I(\phi + \pi)$

$$I_{C_{min}} / I_{C_{max}} \sim \beta \sim \alpha \sim \eta \sim s$$

Simulations of node-lifting in dc SQUID



Node-lifting in Josephson junctions

Josephson junctions:

- Inhomogeneous current distribution *Hard to rule out but the full body of data makes this unlikely*
- 1. Consistent features --- same for all samples and other groups.
- 2. Even-odd effect --- first node is lifted; second node not second node
almost all critical current asymmetries lift ALL nodes
- 3. Node-lifting is very large ~10%
requires large random disorder or systematic variations
- 4. Temperature dependence of the critical current diffraction patterns
node current drops much faster than peak current suggests a change in the supercurrent mechanism, e.g. change in the CPR
- 5. Gate dependence of the critical current
strong suppression at zero field and relative insensitivity at nodes also suggests different supercurrent mechanisms

Node-lifting in Josephson junctions and SQUIDs

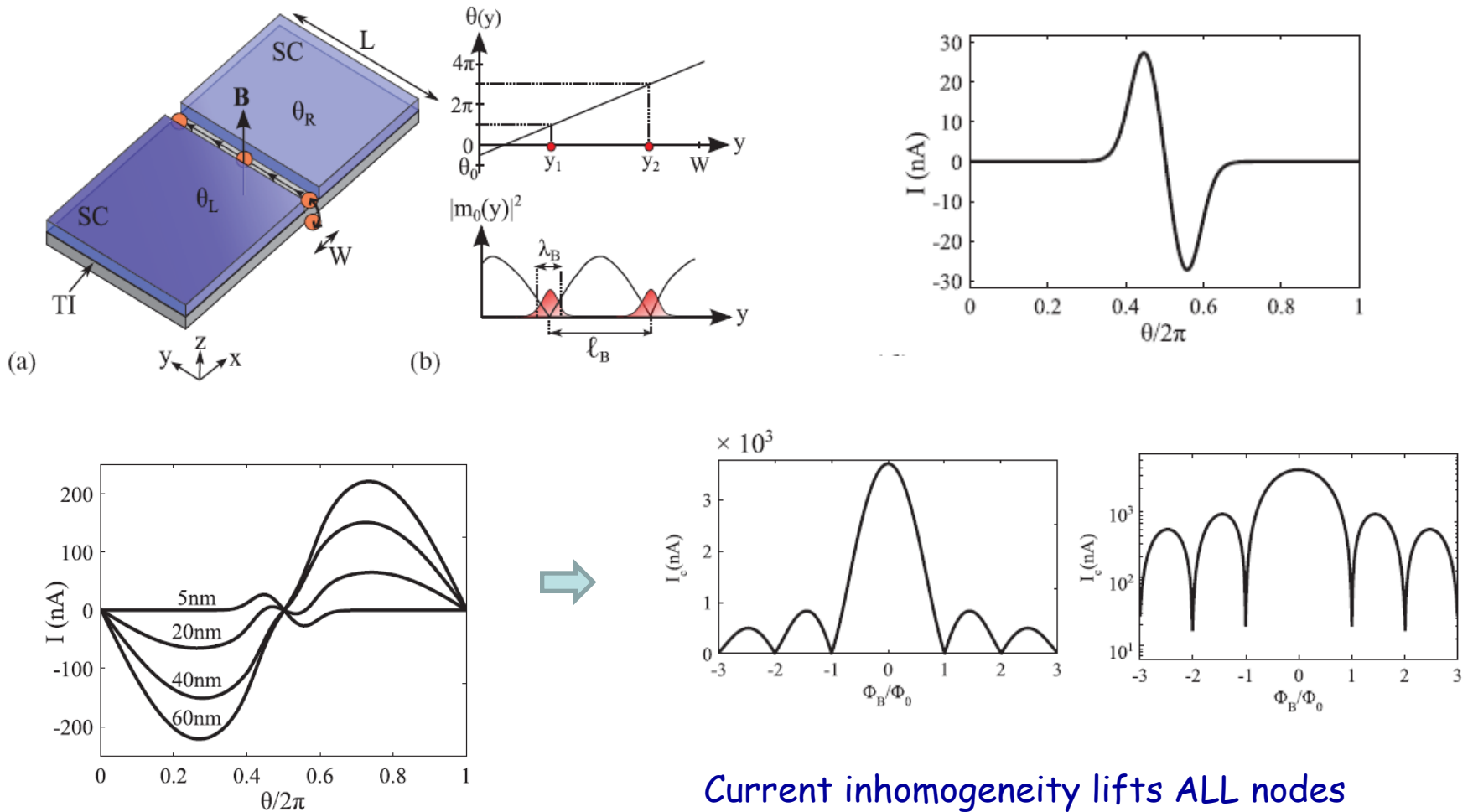
Josephson junctions:

- Inhomogeneous current distribution
- Edge currents due to MF hybridization (Potter-Fu model)

Anomalous supercurrent from Majorana states in topological insulator Josephson junctions

Andrew C. Potter¹ and Liang Fu²

Hybridization at edge for integer flux quanta gives rise to an extra bump in the CPR



Current inhomogeneity lifts ALL nodes

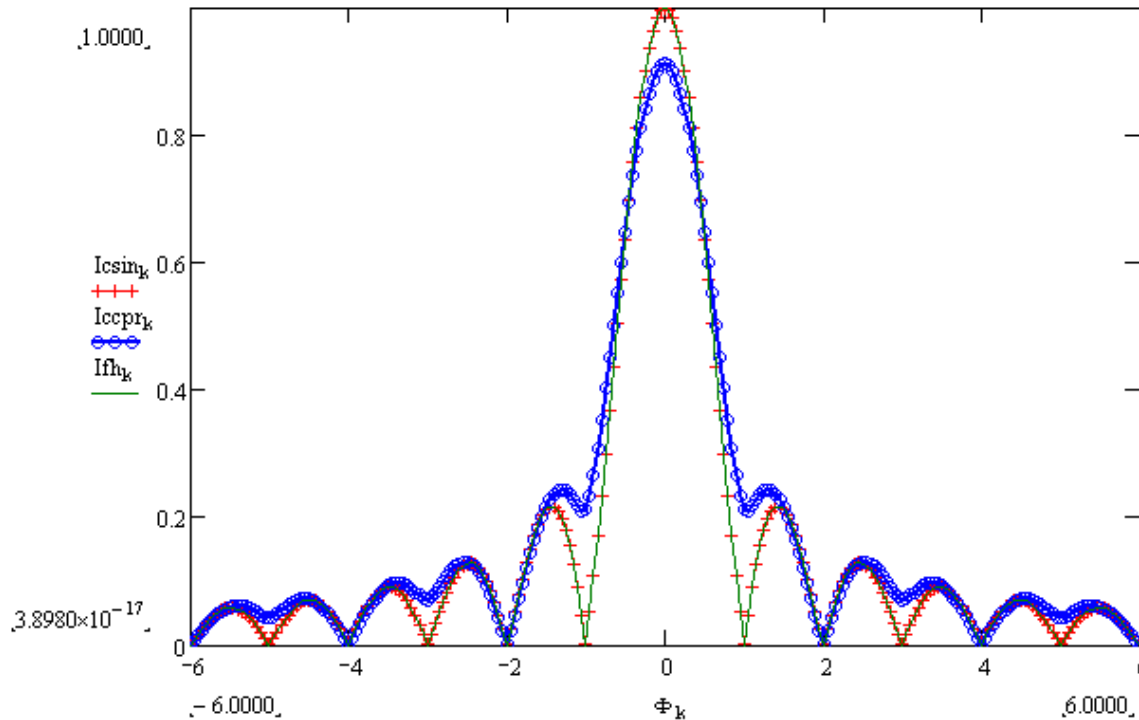
Node-lifting in Josephson junctions and SQUIDs

Josephson junctions:

- Inhomogeneous current distribution
- Edge currents due to MF hybridization (Potter-Fu model)
- $\sin(\phi/2)$ -component in the current-phase relation

Simulations --- Hybrid Current Phase Relation

$$\text{CPR: } I(\phi, V_g) = I_{c1} \sin(\phi) + I_{c2}(V_g) \sin(\phi/2)$$



1st minimum lifted
2nd exactly nulled

Reproduces some key features

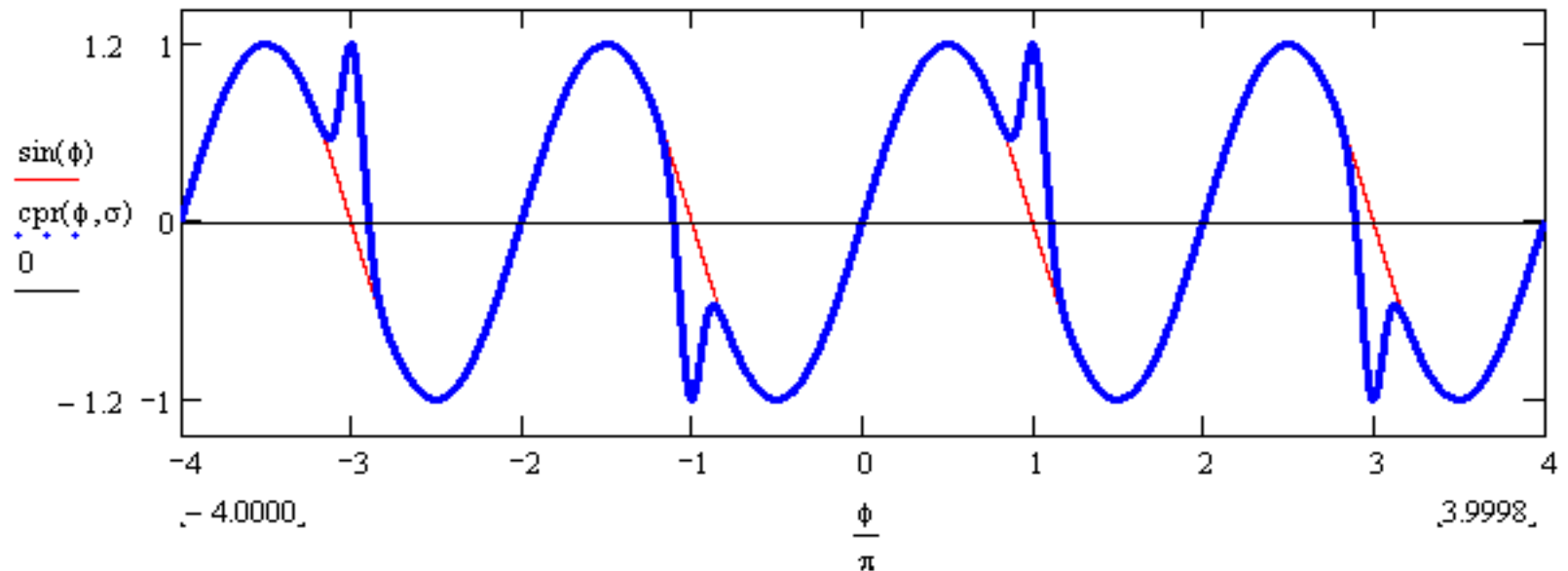
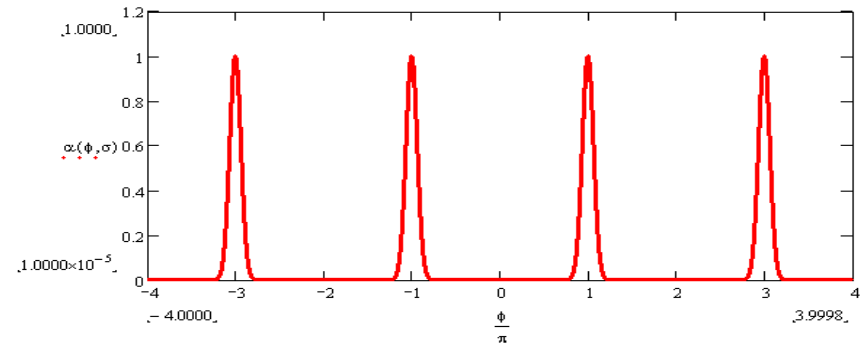
However, this assumes a uniform $\sin(\phi/2)$ -component with should not be the case for Majorana fermions --- only stable when $\phi \sim \pi$

Model --- Current-Phase Relation for S-TI-S junction

Majorana fermions nucleate when/where the phase difference is π

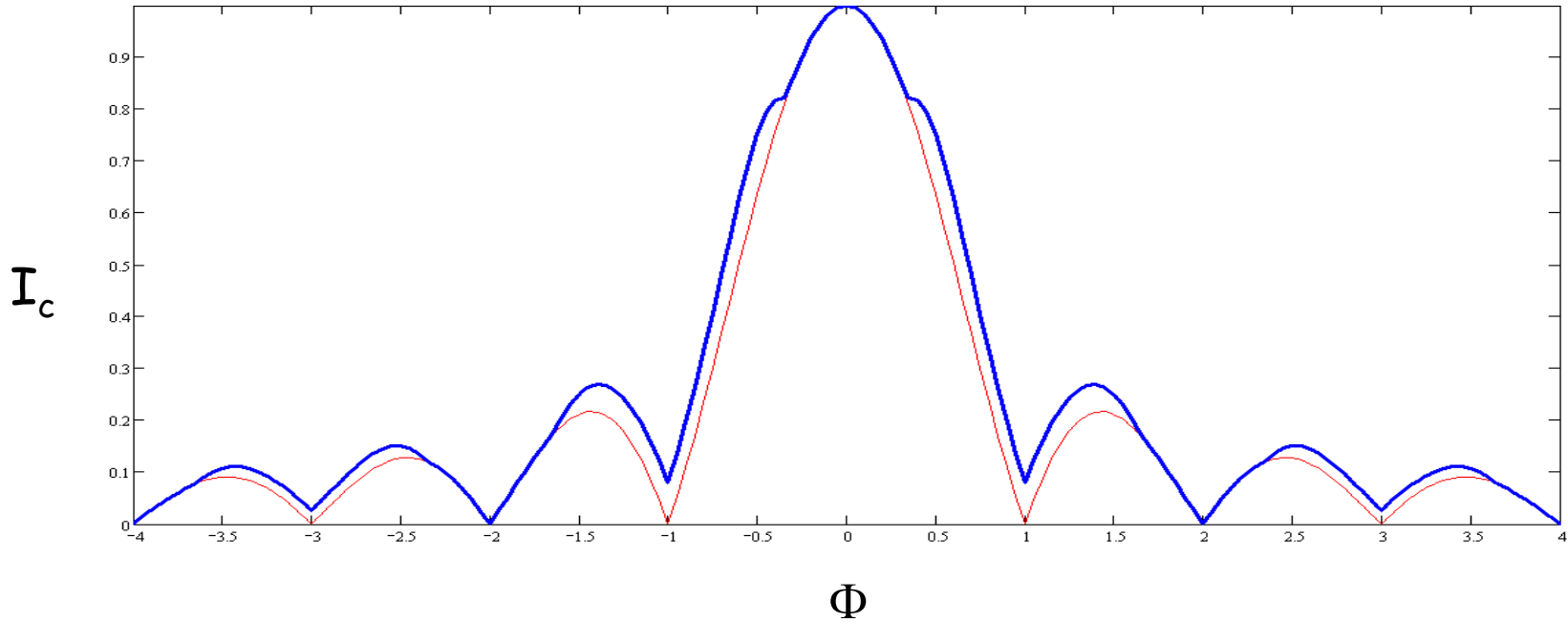
$$I_c(\phi) = (1 - \alpha) \sin(\phi) + \alpha \sin\left(\frac{\phi}{2}\right)$$

Width of the Majorana region will depend on details of the sample



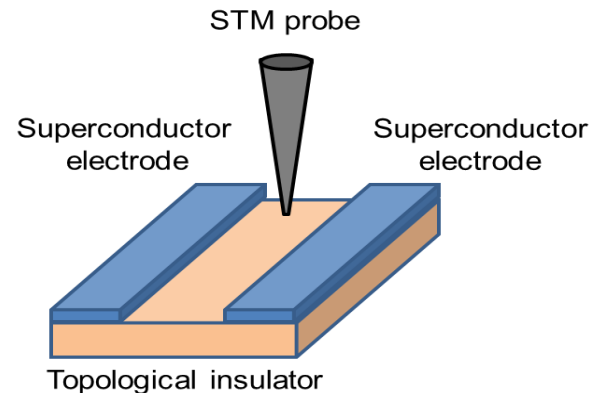
Consider the junction to break up into 1D wires with a $\sin(\phi/2)$ component

Diffraction patterns for S-TI-S junction



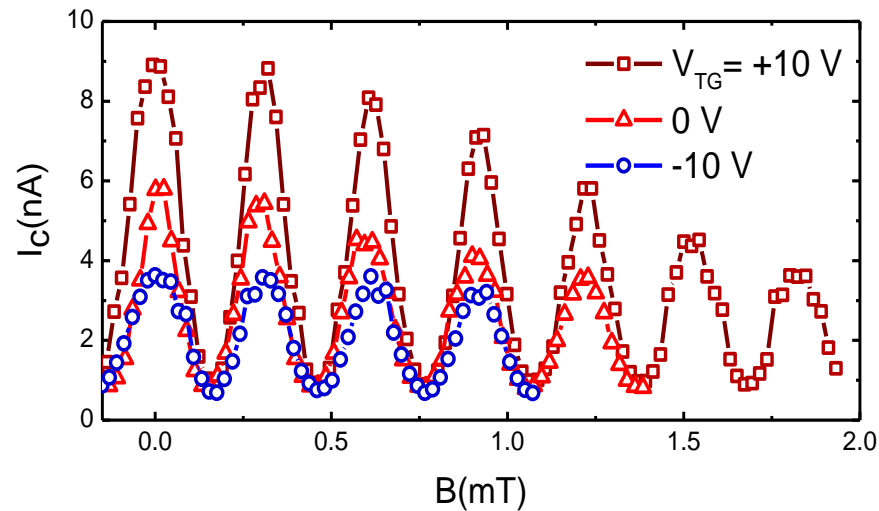
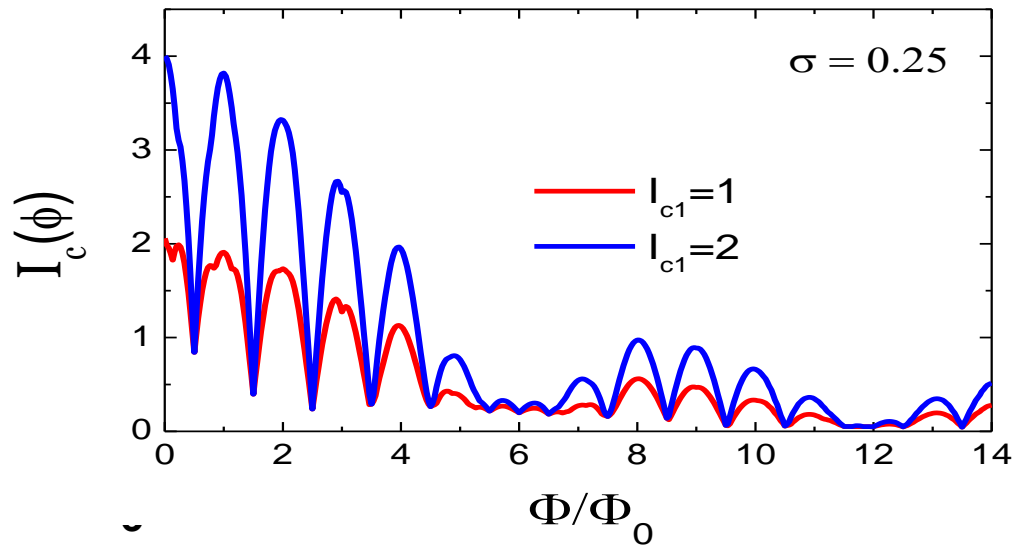
Additional structure onsets when Majorana fermions enter the junction --- this would be a signature of a localized $\sin(\phi/2)$ component in the CPR

Could also look for entry of Majorana fermions via STM spectroscopy



Comparison to CPR model for the SQUID

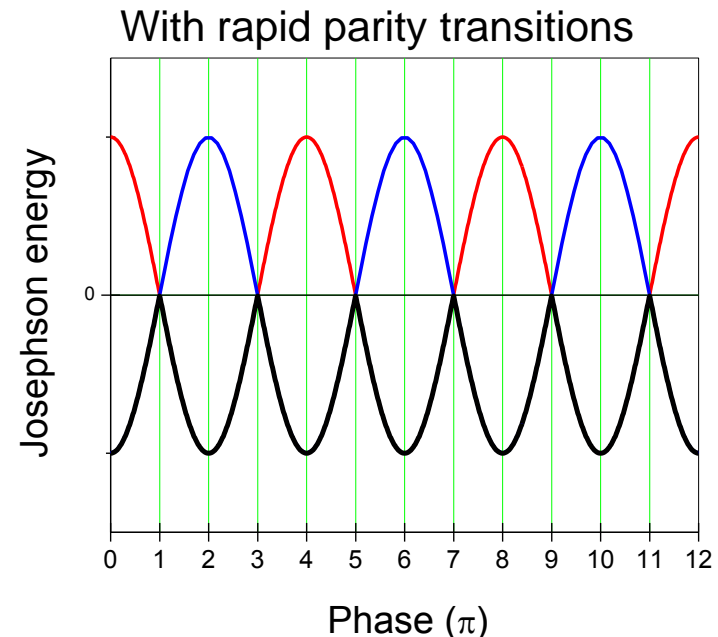
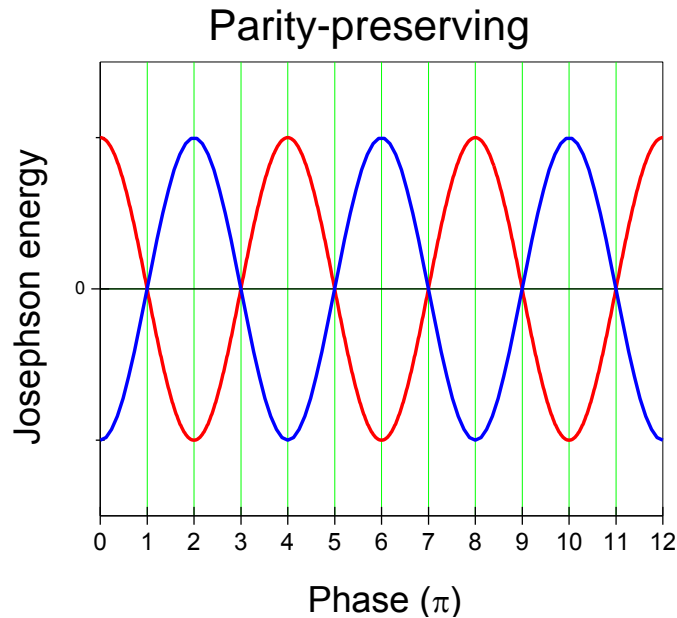
$$I(\phi) = I_{c1} \sin(\phi) + I_{c2} \alpha(\phi, \sigma) \sin(\phi/2)$$



Primary effect of gating is to change $\sin(\phi)$ component

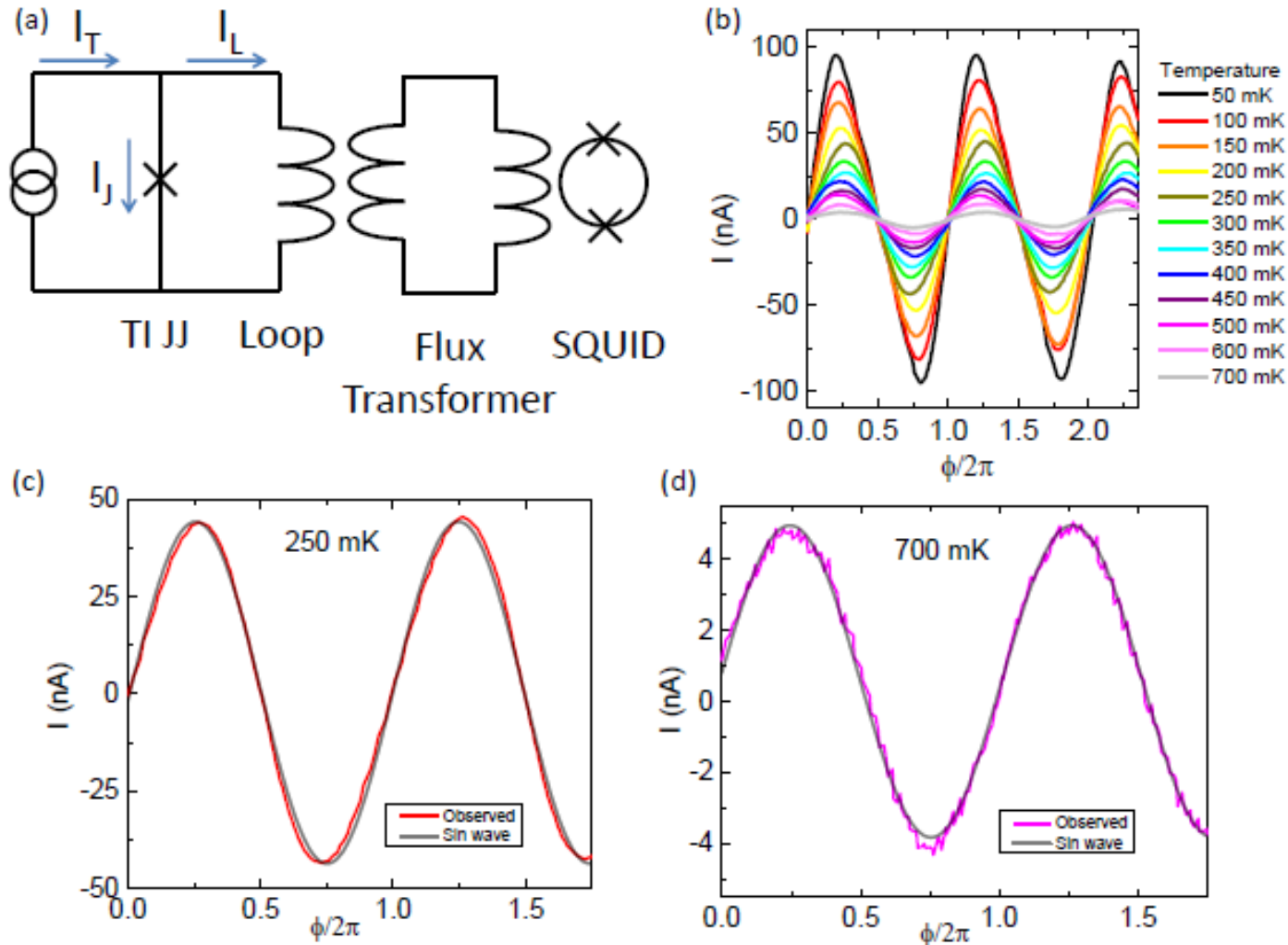
Why can we see the $\sin(\phi/2)$ -component in the CPR?

1. Cancellation of 2π -periodic component by destructive interference at nodes reduces the background \rightarrow effectively a series of 1D channels with a $\sin(\phi/2)$ CPR
2. Dynamical measurement at finite voltage so phase evolves fast enough to avoid parity transitions that suppress the 4π -periodic component. Typical Josephson frequency \sim GHz.



Static measurements of the CPR should not see this

CPR Measurements via Interferometer technique



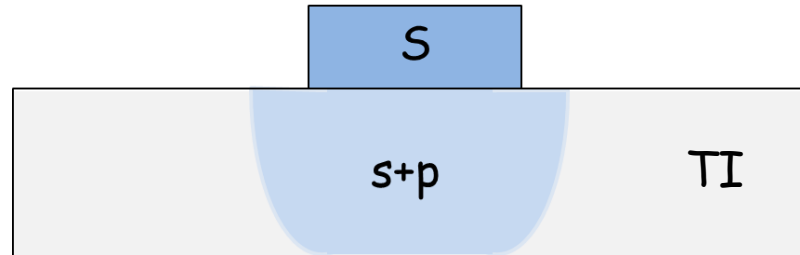
No 4π -periodicity --- expected for a static measurements
Very small skewness but need to measure when gated

Why can we see the $\sin(\phi/2)$ -component in the CPR?

1. Cancellation of 2π -periodic component by destructive interference at nodes reduces the background \rightarrow effectively a series of 1D wires
2. Dynamical measurement at finite voltage so phase evolves fast enough to avoid parity transitions that suppress the 4π -periodic component
3. Need to measure parity lifetime to determine how fast we need to perform braiding operations, e.g. frequency-dependent CPR
4. The sign of the $\sin(\phi/2)$ -component encodes the Majorana fermion pair parity --- route to measuring the parity in circuits.

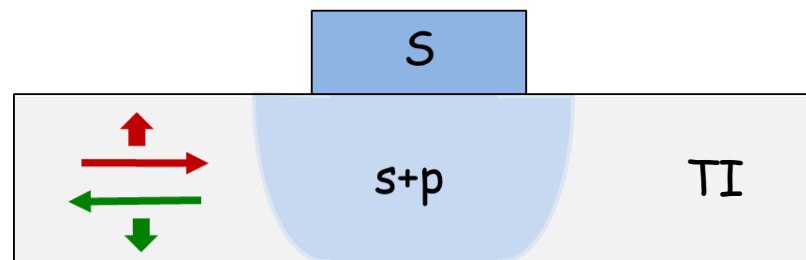
**Interferometry experiments
in hybrid Nb-Bi₂Se₃ structures**

Order parameter symmetry of the proximity-induced superconductivity in a topological insulator



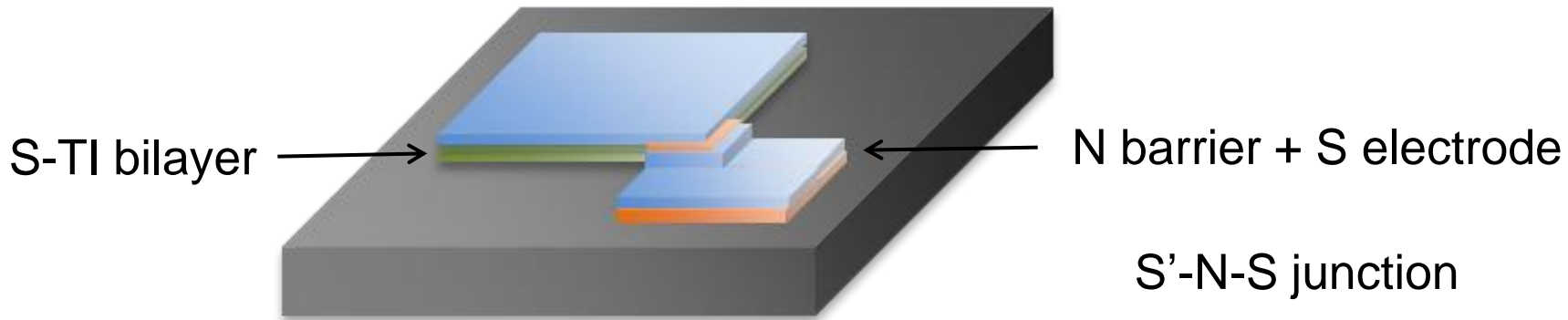
$$\Delta(s+p) = \Delta(s) + (\uparrow) \Delta(p_x + ip_y) + (\downarrow) \Delta(p_x - ip_y)$$

Current \rightarrow spin-momentum locking \rightarrow spin-selected chiral order parameter

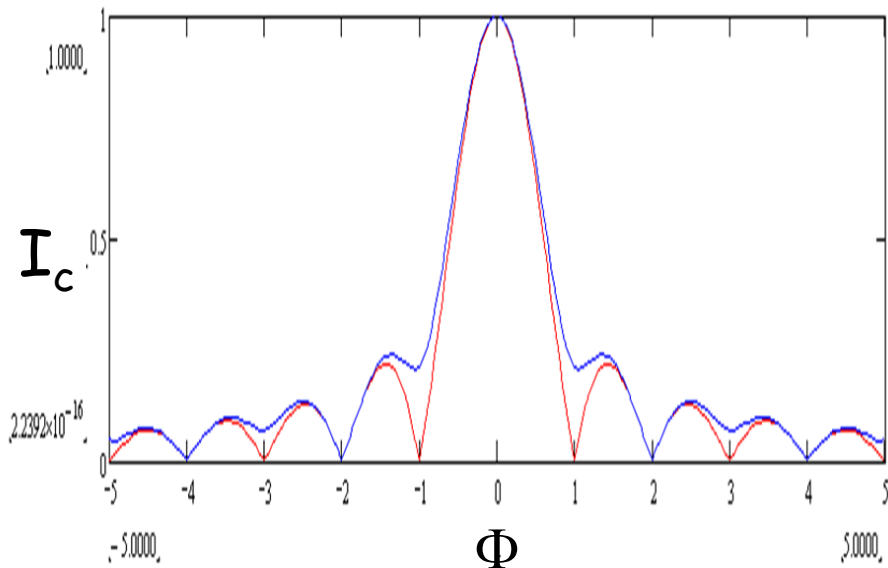


$$\Delta(\uparrow) = \Delta(s) + \Delta(p_x + ip_y) \quad \Delta(\downarrow) = \Delta(s) + \Delta(p_x - ip_y)$$

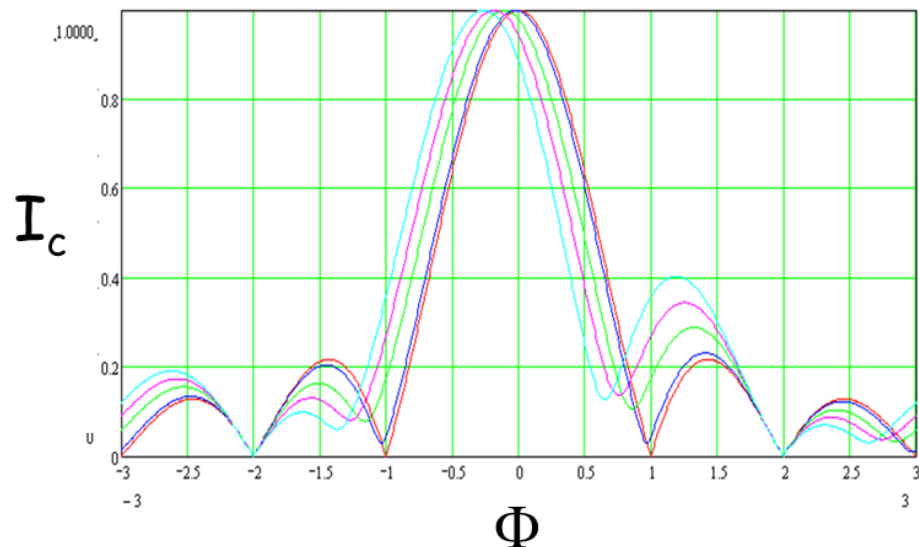
Approach: Josephson interferometry of an S-TI bilayer (corner SQUID experiment)



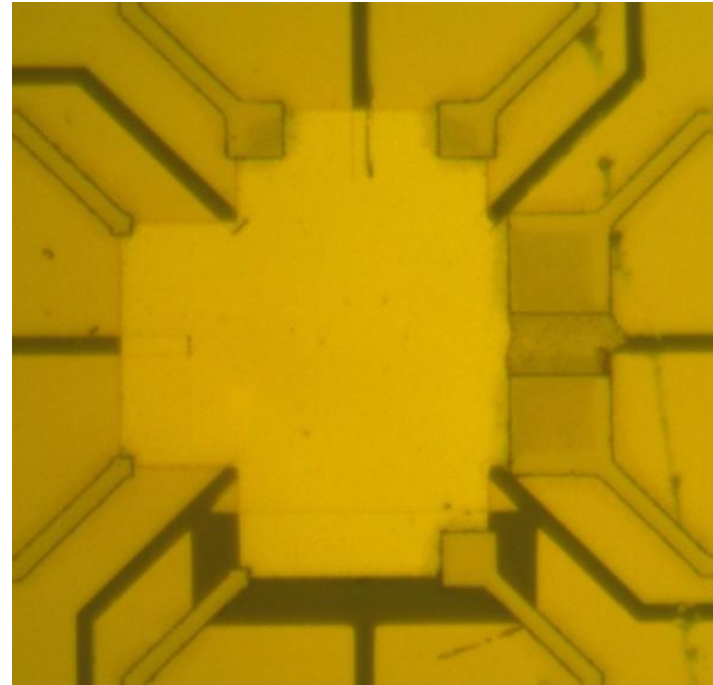
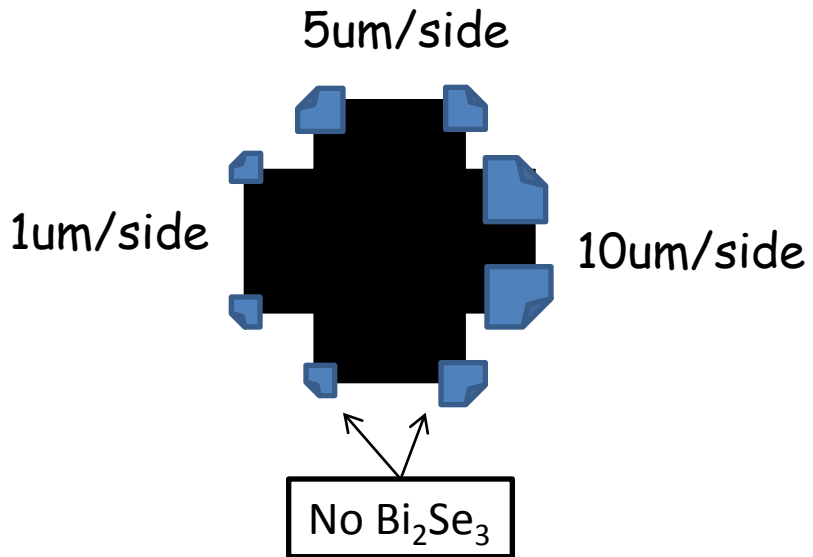
$s + p_x$



$s + \alpha (p_x + ip_y)$



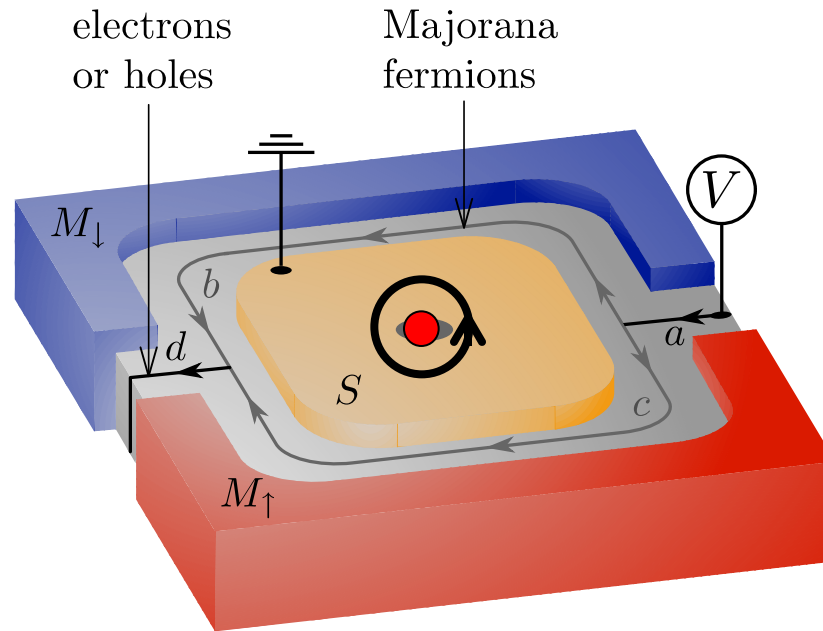
Sample design and fabrication



Sample Side View



Majorana Interferometry



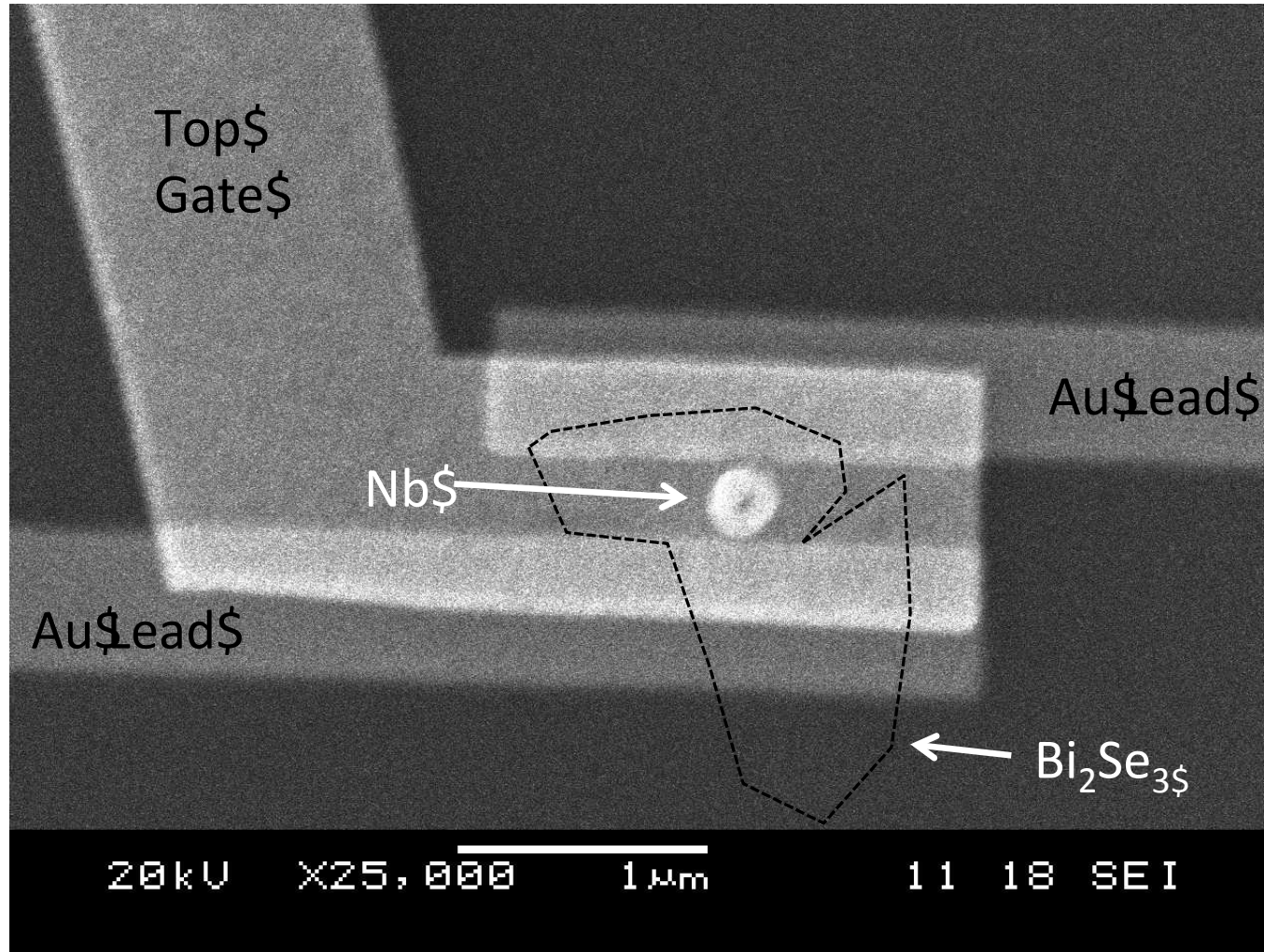
$$G(V) = \frac{2e^2}{h} |S_{he}(eV)|^2 = \frac{2e^2}{h} \sin^2\left(\frac{n_v \pi}{2} + \frac{eV \delta L}{2\hbar v_m}\right).$$

Vortex trapped in SC films introduces a phase shift

Fu and Kane, Phys. Rev. Lett. **102**, 216403 (2009).

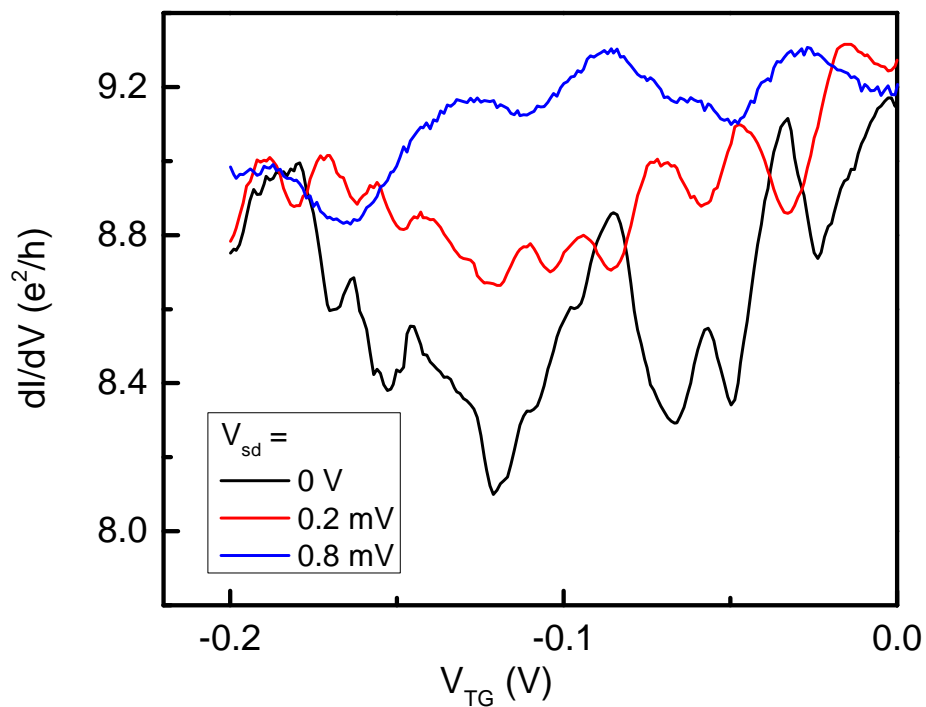
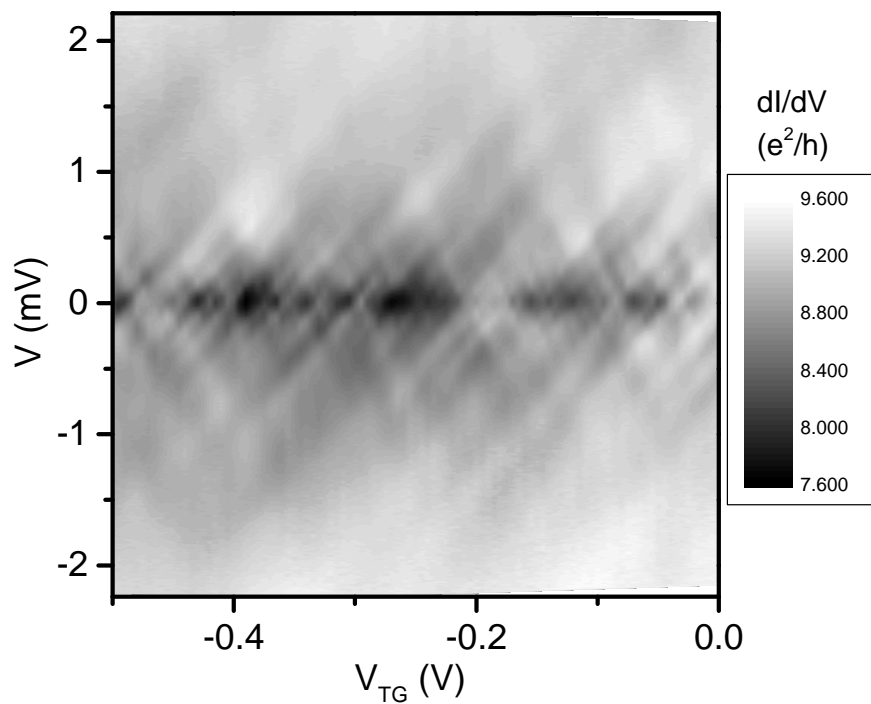
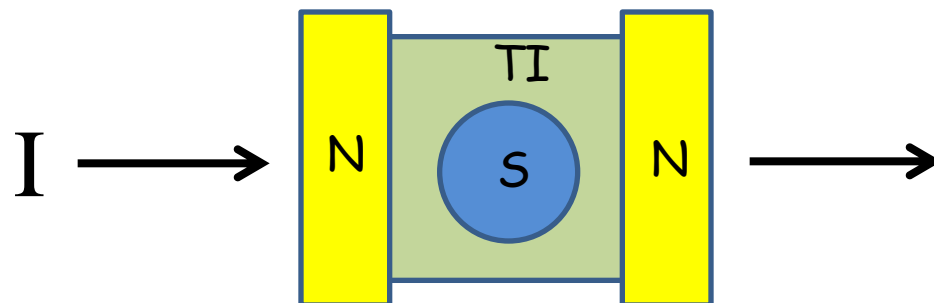
Akhmerov, Nilsson, and Beenakker, Phys. Rev. Lett. **102**, 216404 (2009).

Aharonov-Bohm Interferometer



~200 nm wide niobium disk in the middle of a gold-TI-gold junction.

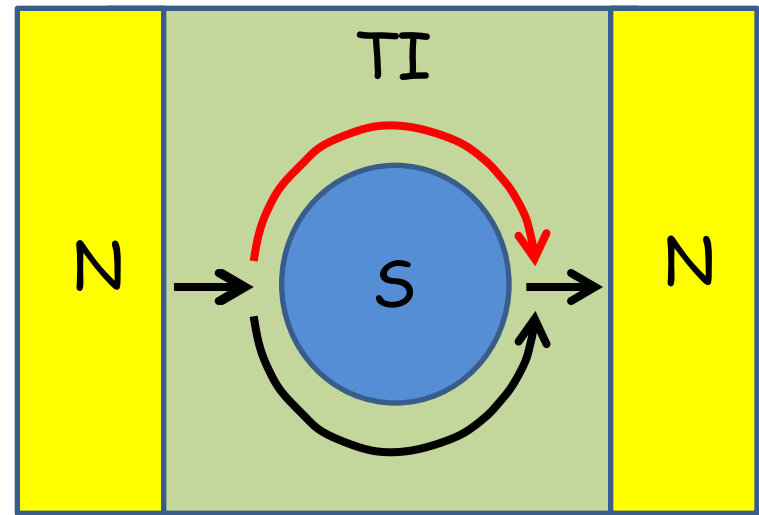
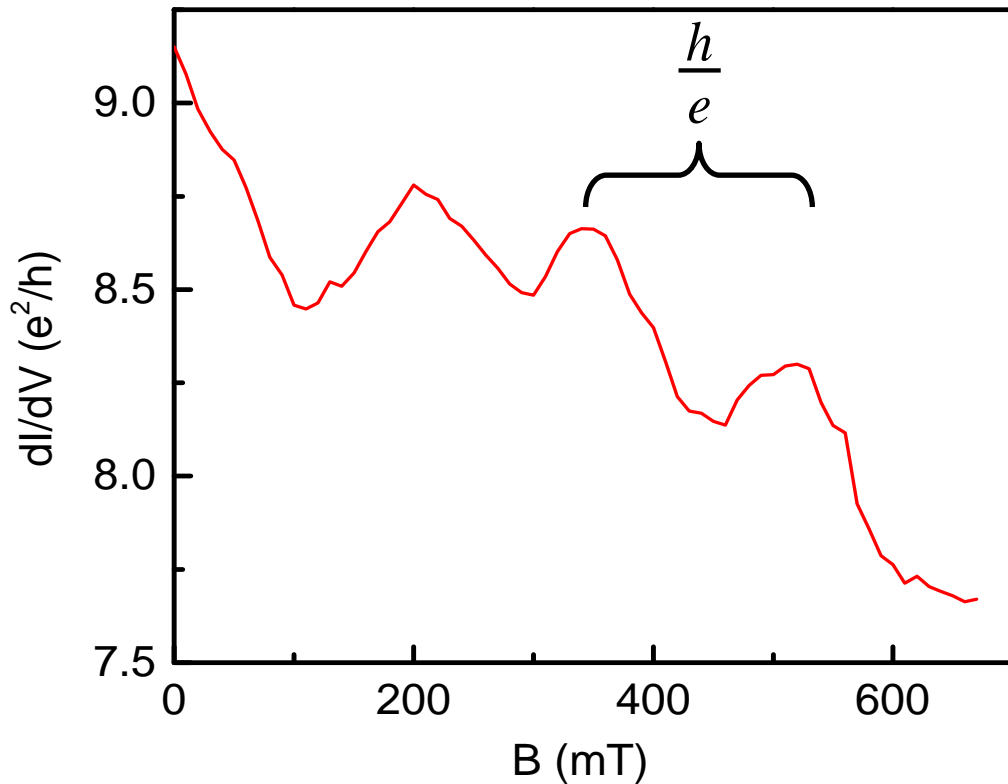
Zero Field Transport



See usual Fabry-Perot and Andreev bound state resonances

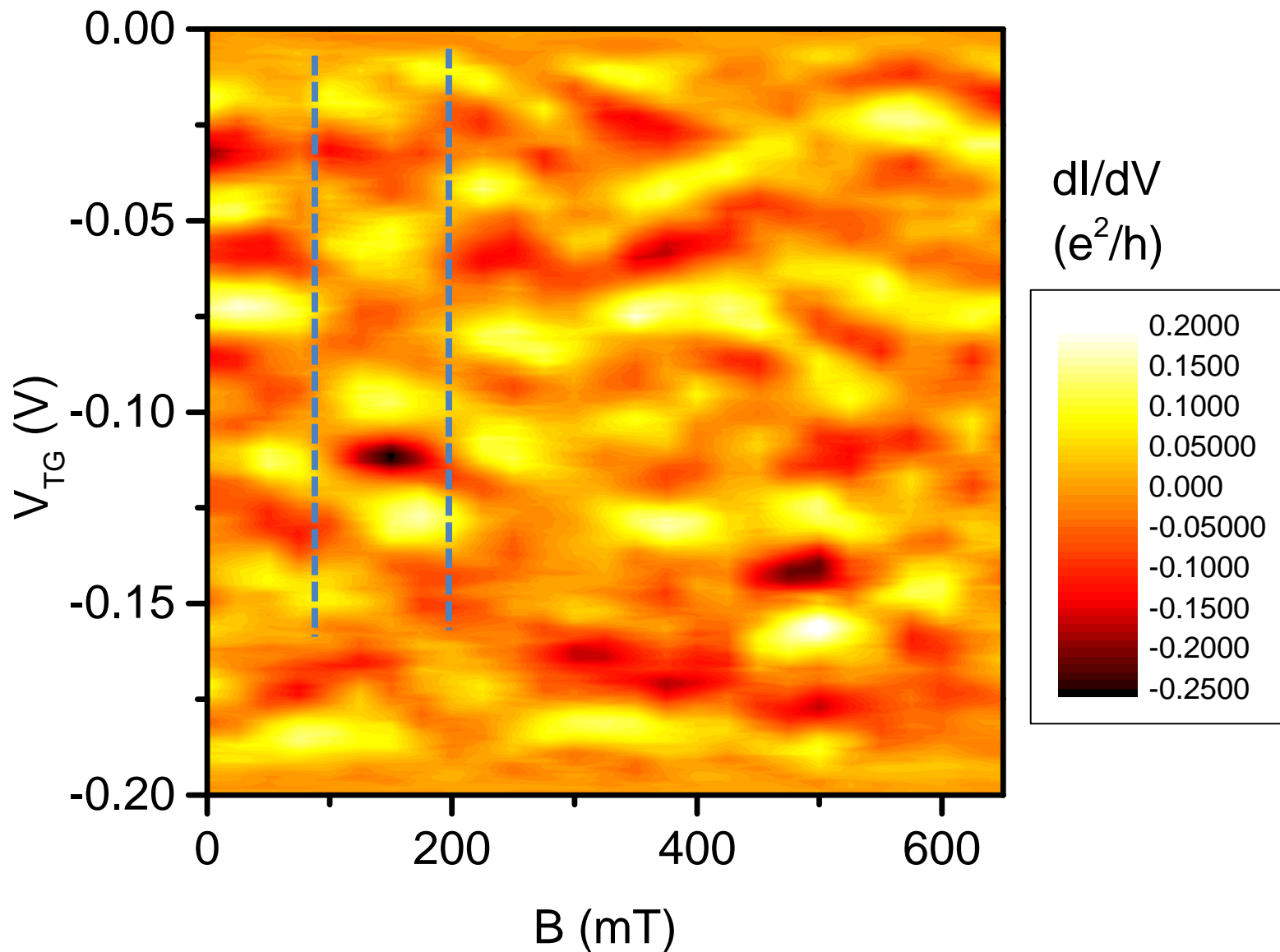
Finite Field Transport

Observe conductance oscillations --- Aharonov-Bohm interference



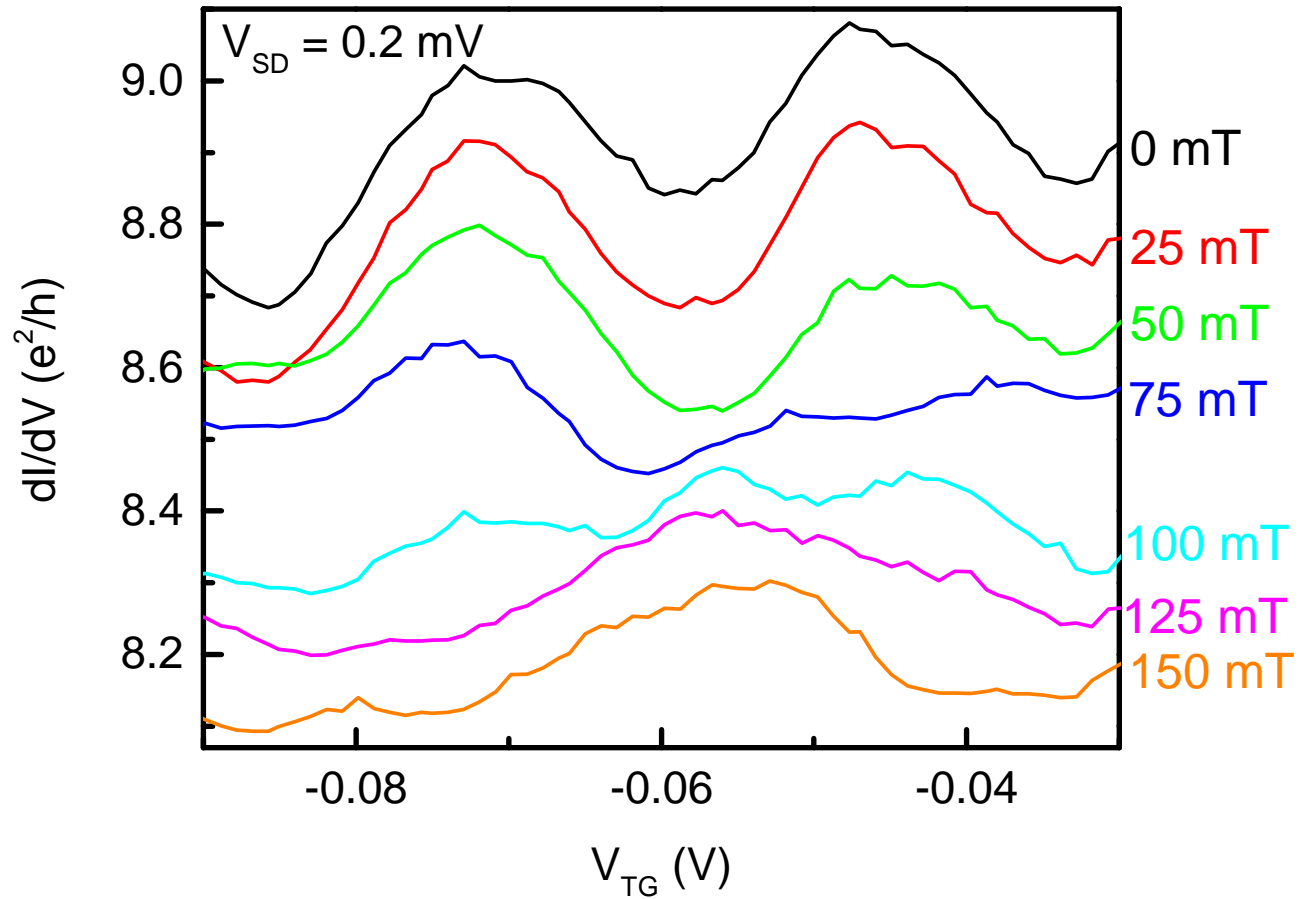
- Period $\sim 1 \Phi_0$ in area of superconducting dot
- Oscillations vanish if no multiply-connected path
- Suggests highly-conducting channels at the edge of the island
- Speculate that the magnetic field Meissner-screened from the island suppresses proximity-induced SC and creates a topological channel for MFs

Conductance vs. Gate voltage and Field Sweeps



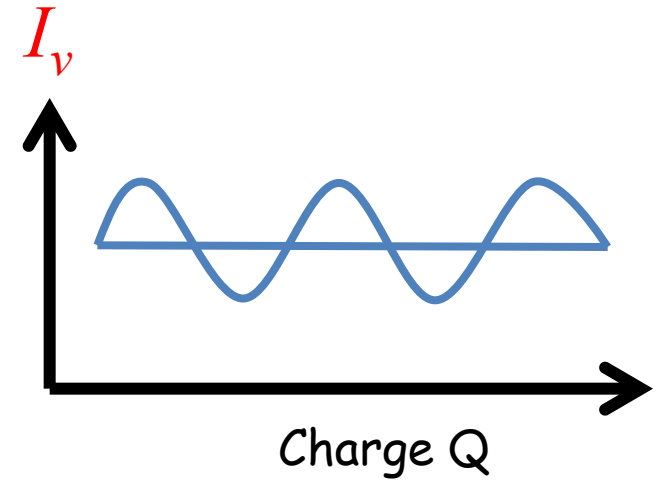
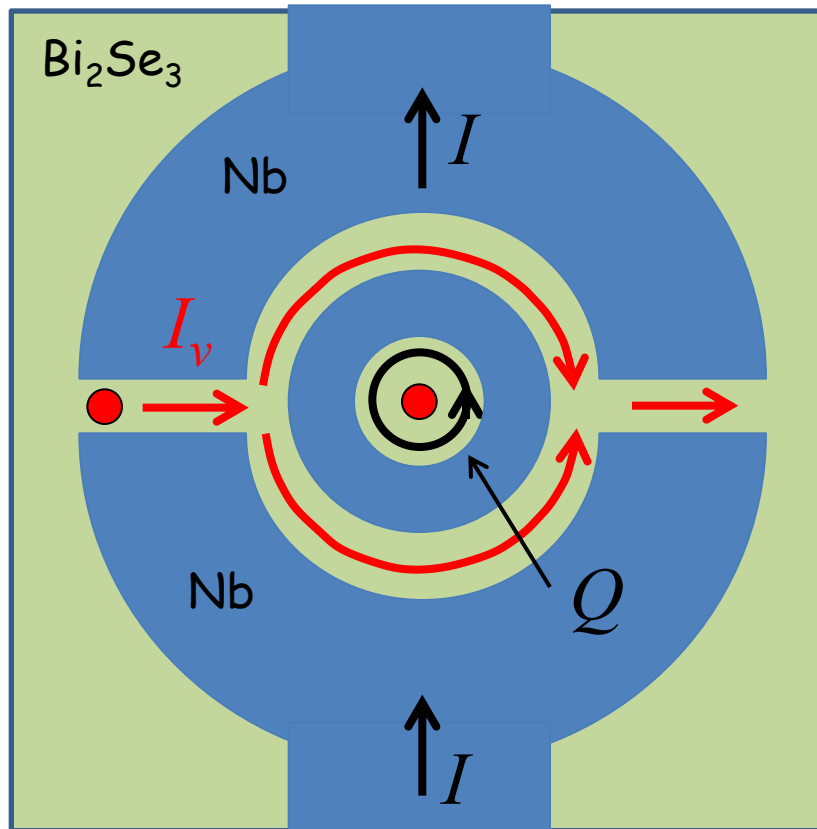
Checkerboard pattern.

Abrupt phase shift in gate oscillation vs. magnetic field



Could arise from a vortex + Majorana fermion entering the superconducting island

Majorana Interferometry via the Aharonov-Casher effect



Das Sarma et al., PRB **73**, 220502R (2006);
Grosfeld et al., PRB **83**, 104513 (2011);
Grosfeld and Stern, PNAS **108**, 11810 (2011).
Alicea, Rep. Prog. Phys. **75**, 076501 (2012).

Observation of the Aharonov-Casher Effect for Vortices in Josephson-Junction Arrays

W. J. Elion, J. J. Wachters, L. L. Sohn, and J. E. Mooij

Department of Applied Physics, Delft University of Technology, P.O. Box 5046, 2600 GA Delft, The Netherlands

(Received 26 March 1993)

We have observed quantum interference of vortices in a Josephson-junction array. When vortices cross the array along a doubly connected path, the resultant resistance oscillates periodically with an induced charge enclosed by the path. This phenomenon is a manifestation of the Aharonov-Casher effect. The period of oscillation corresponds to the single electron charge due to tunneling of quasiparticles.

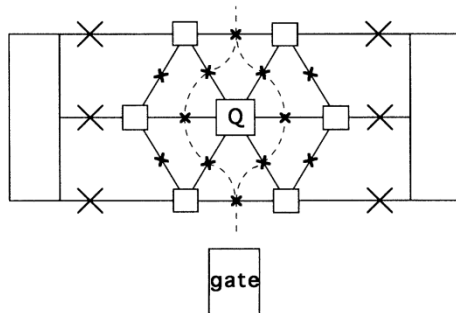


FIG. 1. Schematic layout of the sample. Rectangles are superconducting aluminum islands and crosses denote Josephson junctions. The junctions in the hexagon have a 3 times smaller junction area than the junctions that couple the array to superconducting current and voltage contacts. The dashed lines picture the possible vortex paths.

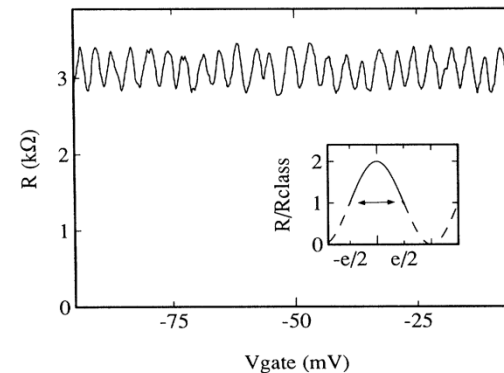
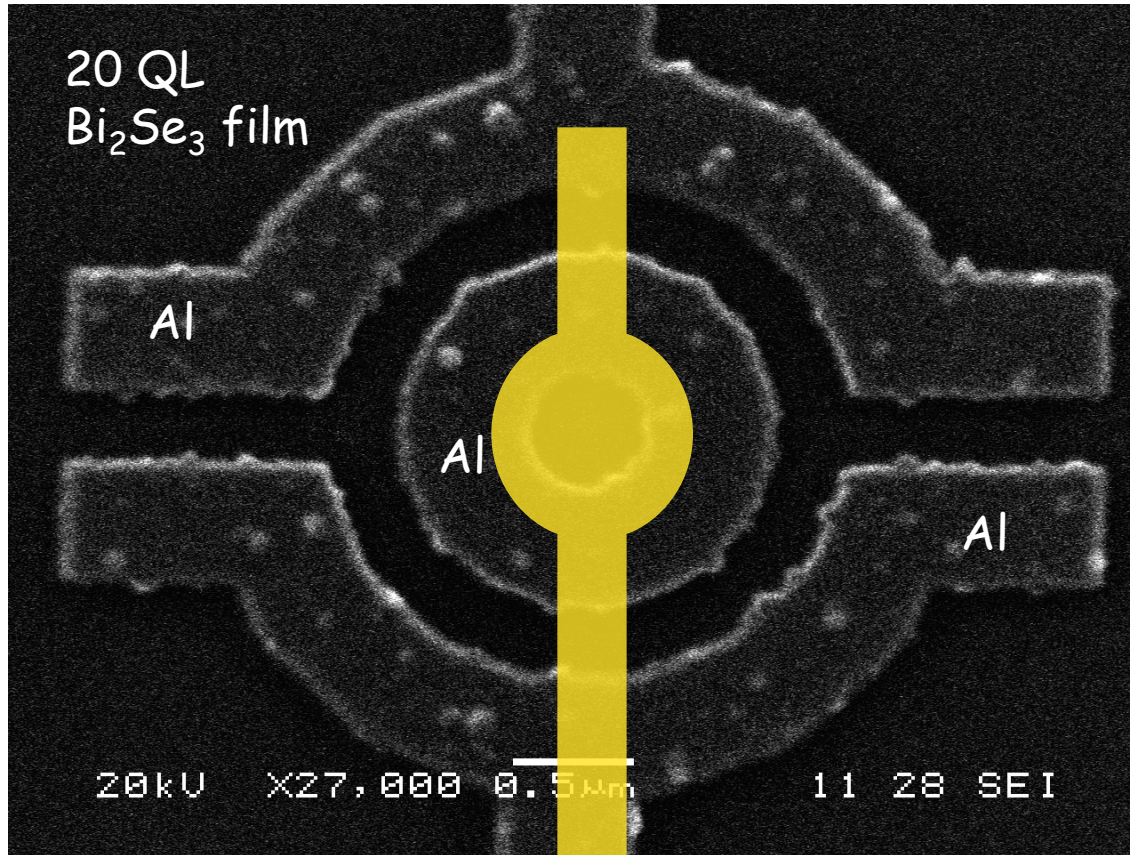


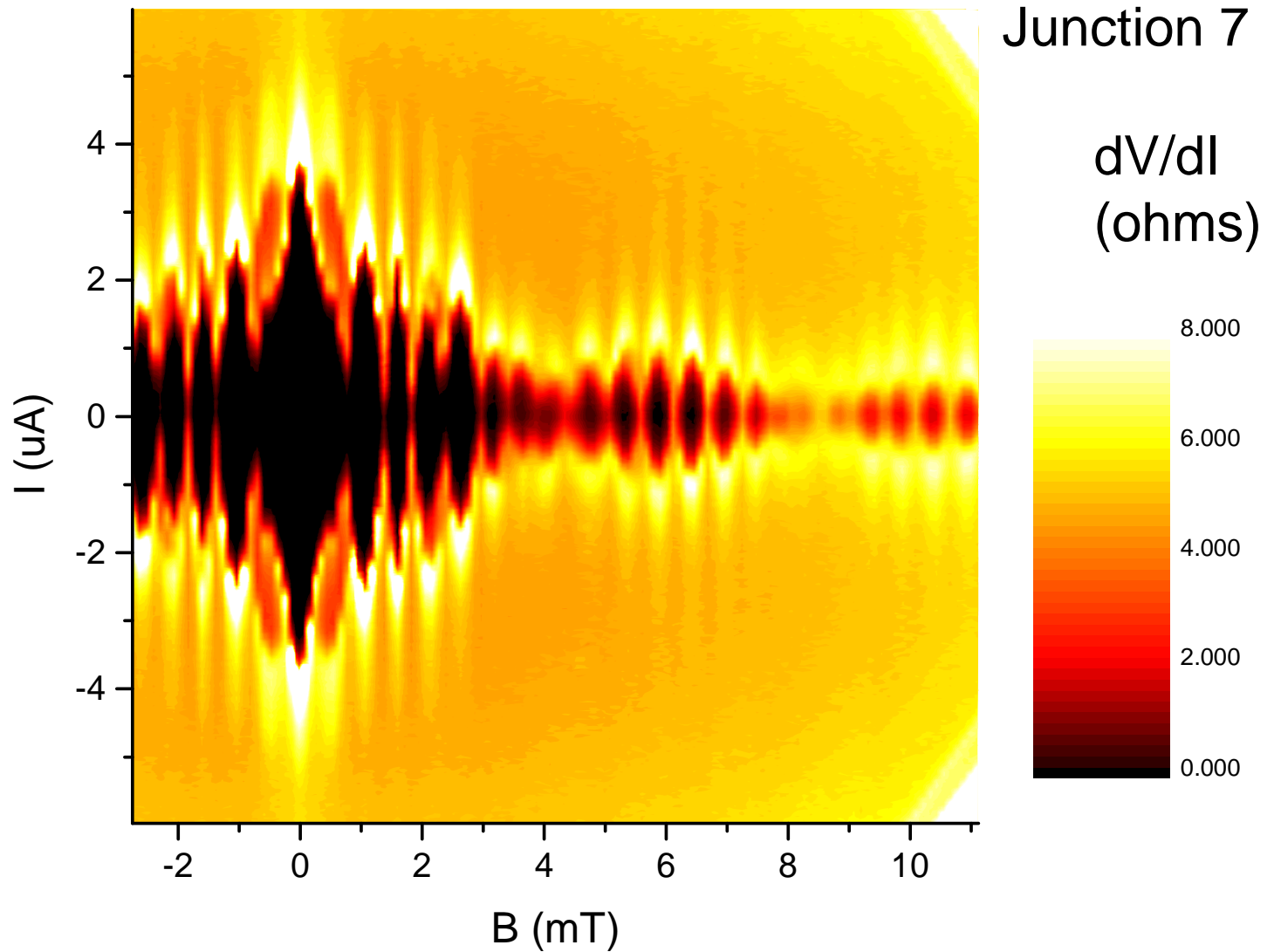
FIG. 2. Differential resistance as a function of gate voltage in a field of $120 \mu\text{T}$. Bias current is 5 nA with 0.25 nA modulation amplitude. Inset: Expected resistance as a function of charge on the center island, normalized to the classical resistance. At $Q = \pm e/2$ quasiparticle tunneling occurs to minimize the charging energy. On sweeping the gate voltage, the charge remains in the range $[-e/2, e/2]$.

Aharonov-Casher Interferometer



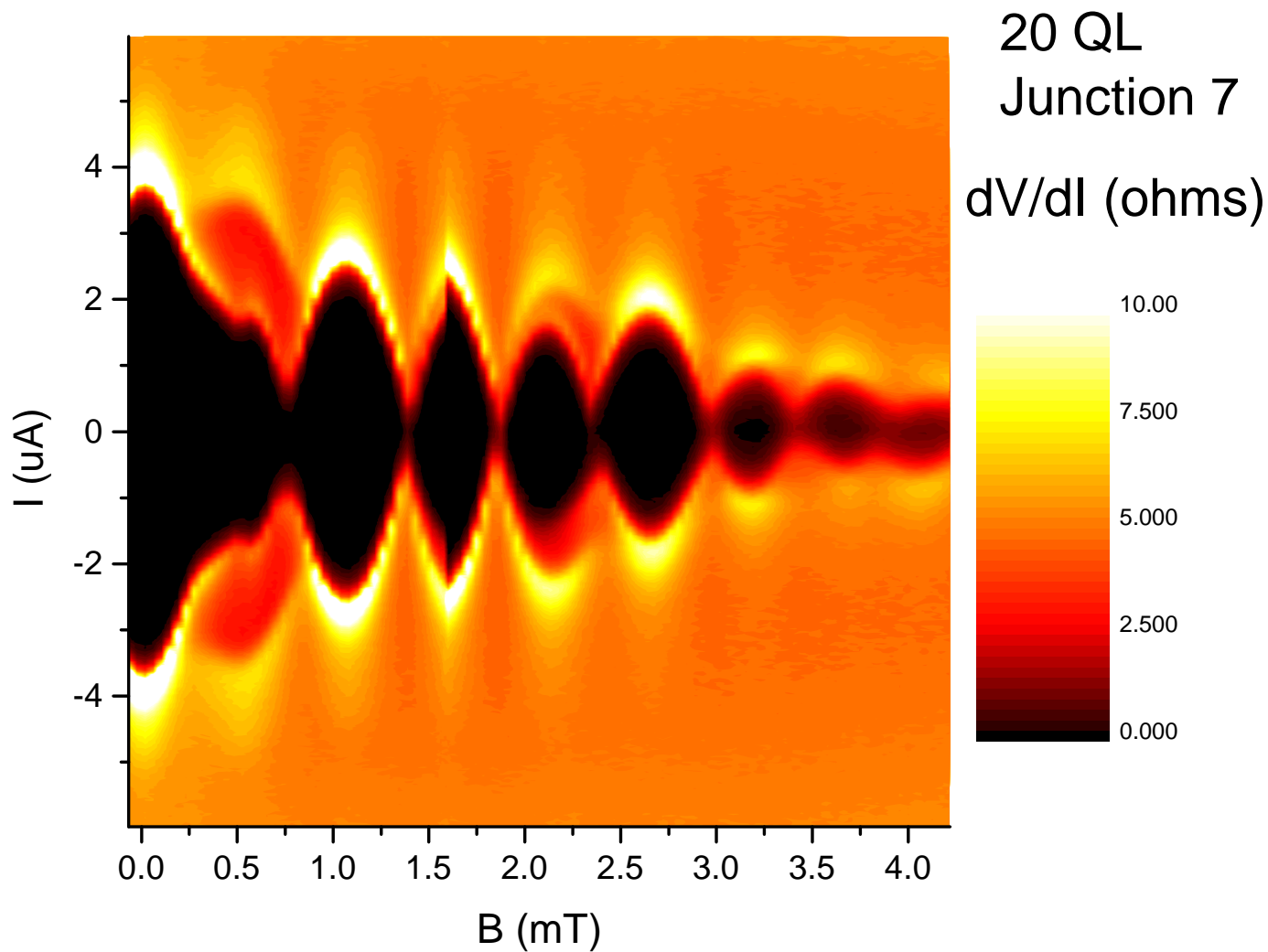
Top Gate

SQUID modulation pattern



Nodes = $h/2e$ flux in the junction regions (with flux focusing.)

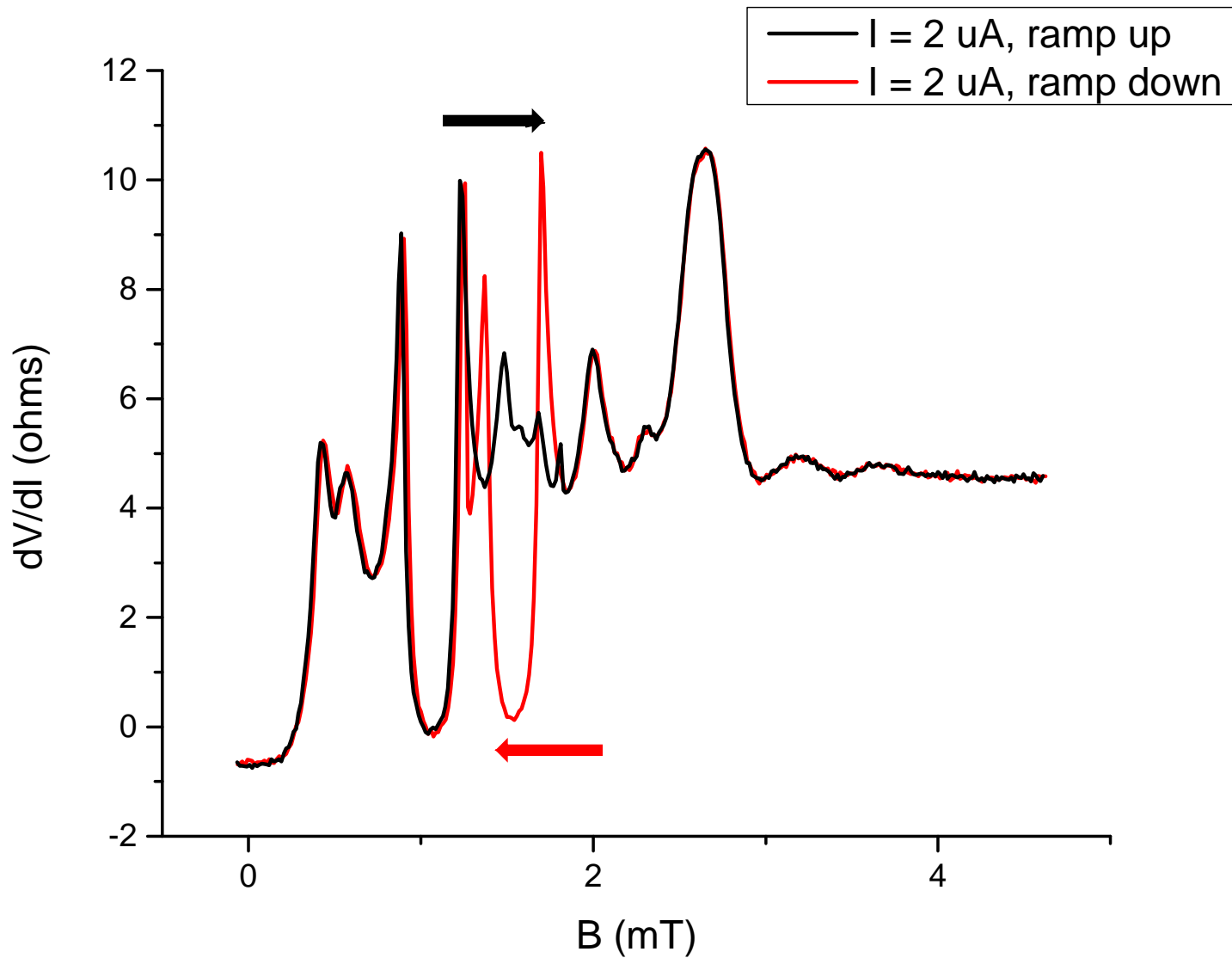
SQUID modulation pattern



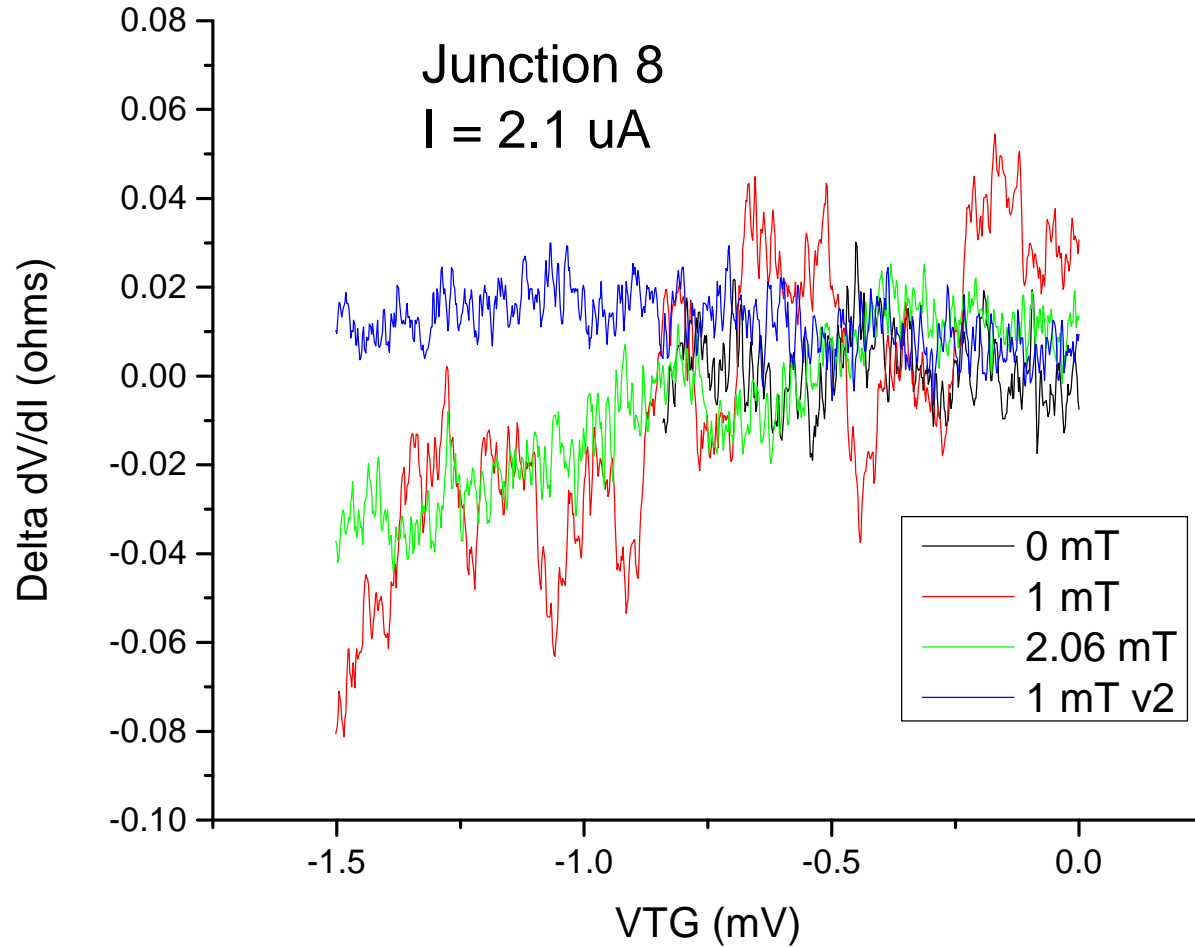
Period of oscillations = $h/2e$ flux in central region

Discrete jumps observed --- vortex entry into central hole?

Hysteresis indicating flux entry



Aharonov-Casher Oscillations



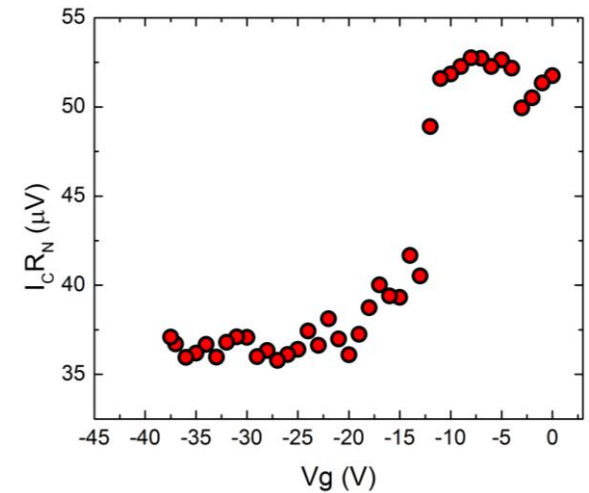
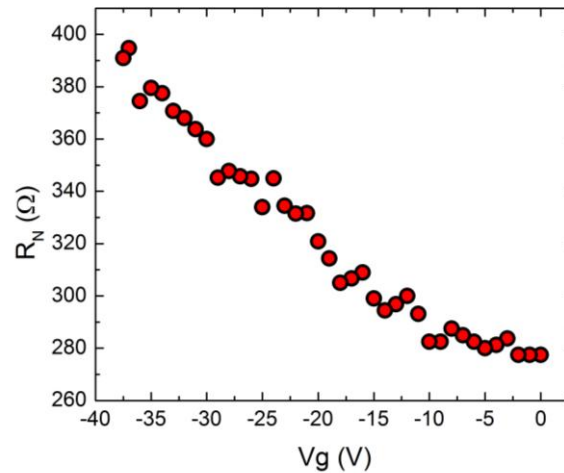
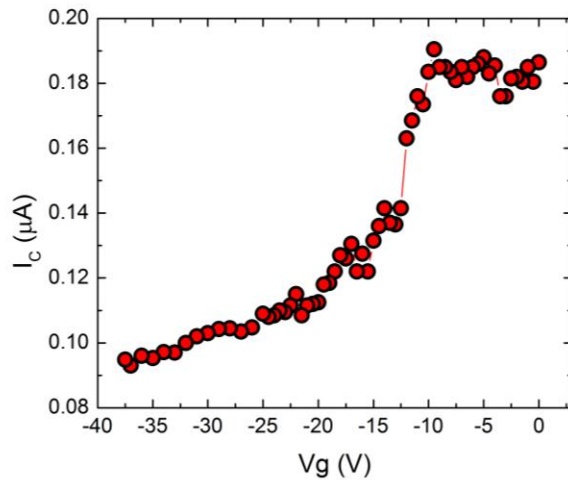
No signs of Aharonov-Casher effect, even at higher magnetic field.

Conclusions

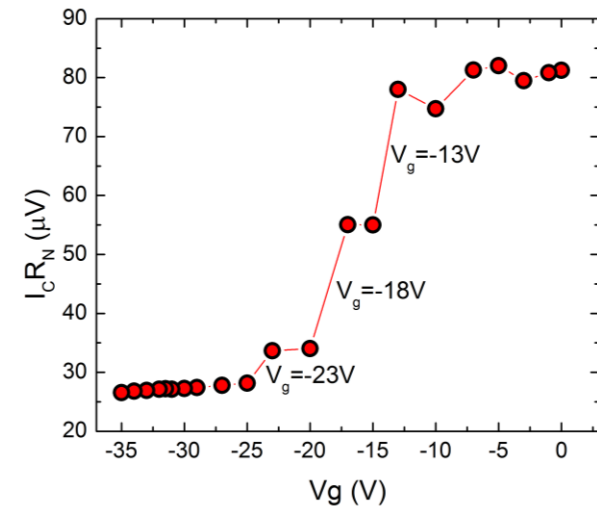
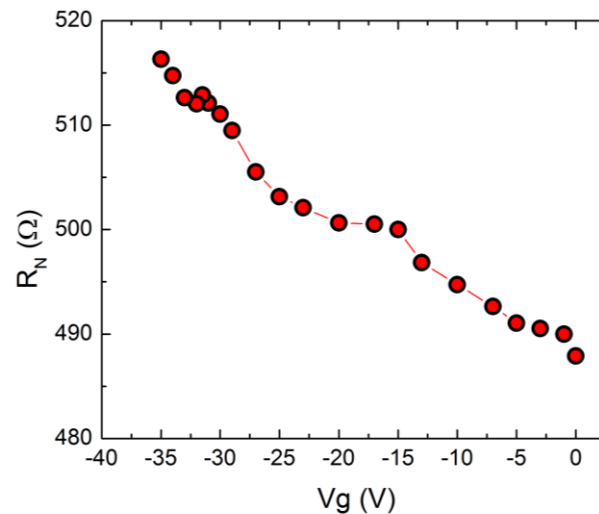
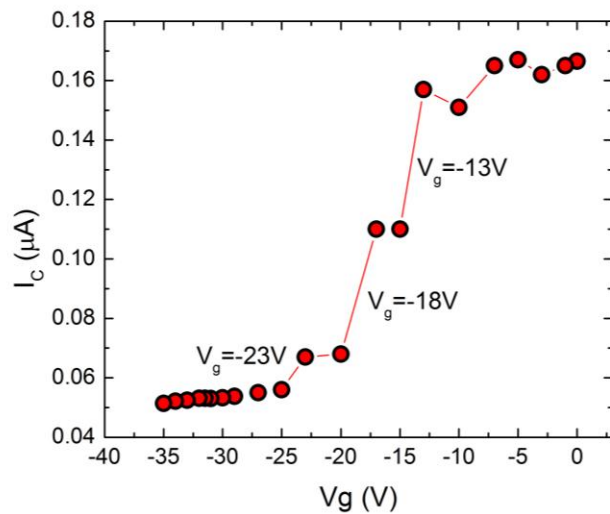
- Lateral S-TI-S may be an attractive system for realizing topological states and Majorana fermions
- Evidence for MFs via 4π -periodic component in the CPR
- Allows MFs to be nucleated and manipulated via phase, currents, and voltages
- Allows parity to be measured via sign of the $\sin(\phi/2)$ term
- Platform for interferometry experiments.

I_c , R_N , and $I_c R_N$ vs. V_g

Sample: 6QL $l=0.3\mu\text{m}$ $w=0.5\mu\text{m}$

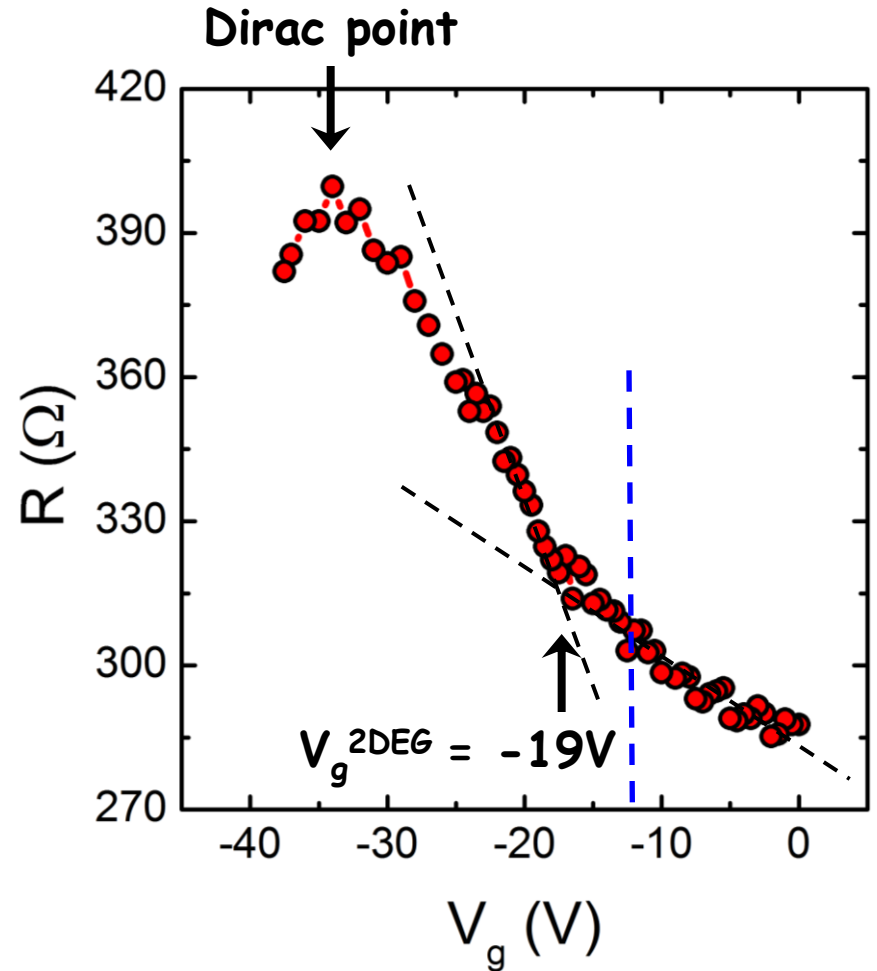
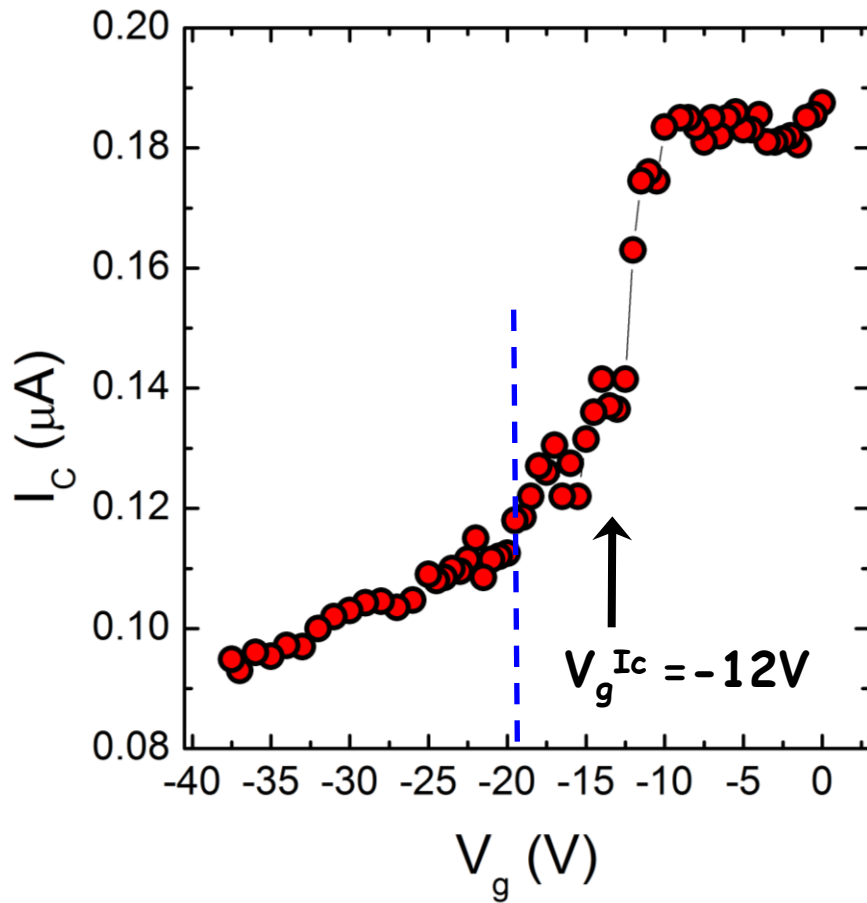


Sample: 30QL $l=0.35\mu\text{m}$ $w=1.0\mu\text{m}$



Steps due to moving Fermi level through discrete surface bands?

Gate Voltage dependence -- critical current and resistance



$$|V_g^{I_c}| < |V_g^{2\text{DEG}}|$$

Jump in I_c

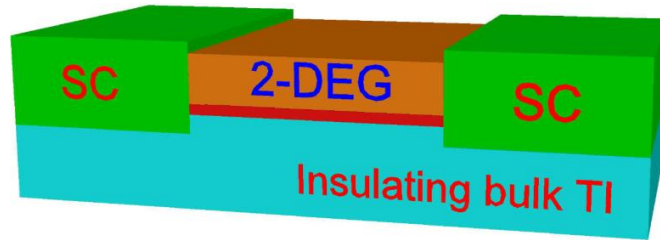
Inflection point in resistance \rightarrow
depopulation of 2DEG

Theoretical Model -- Series of papers by Pouyan Ghaemi

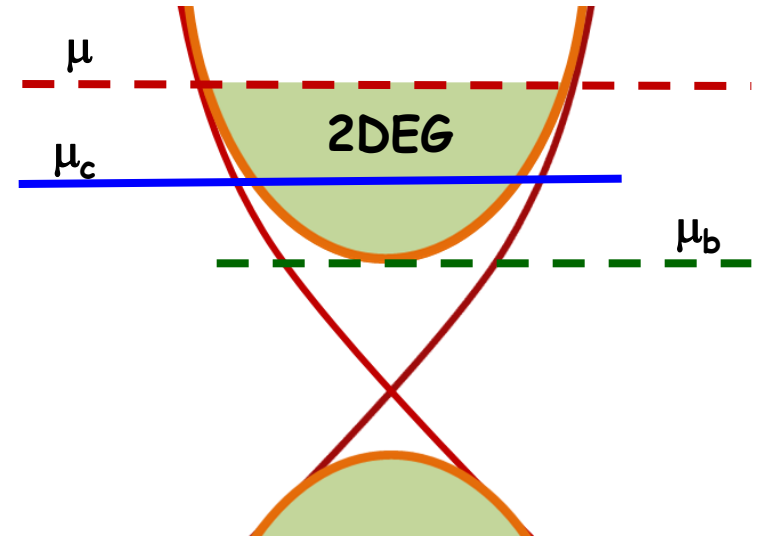
Defines a critical chemical potential for topological phase transition = $\mu_c > \mu_b$
(μ_b = bottom of 2DEG conduction band)

Low gate voltage:

- Fermi energy in conduction band
- Topological surface state buried

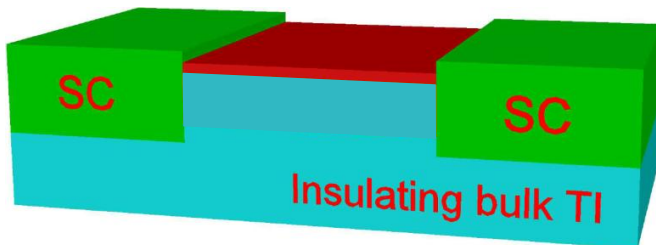


$$\mu > \mu_c$$

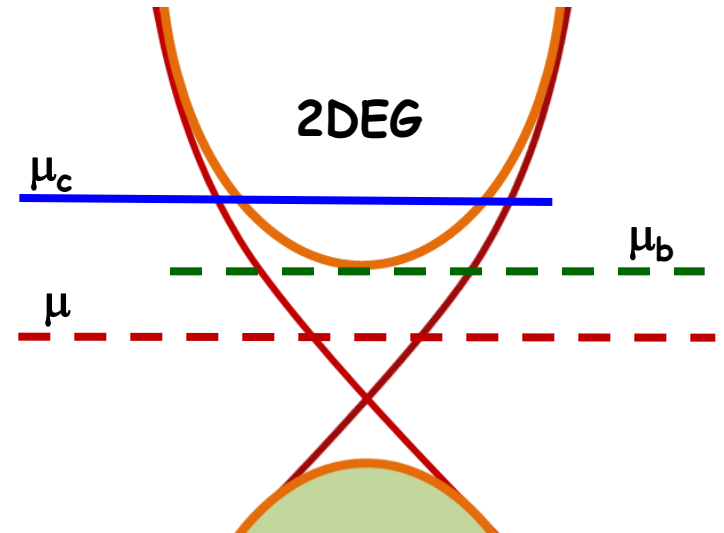


High (negative) voltage:

- Fermi energy in the band gap
- Topological surface state on surface

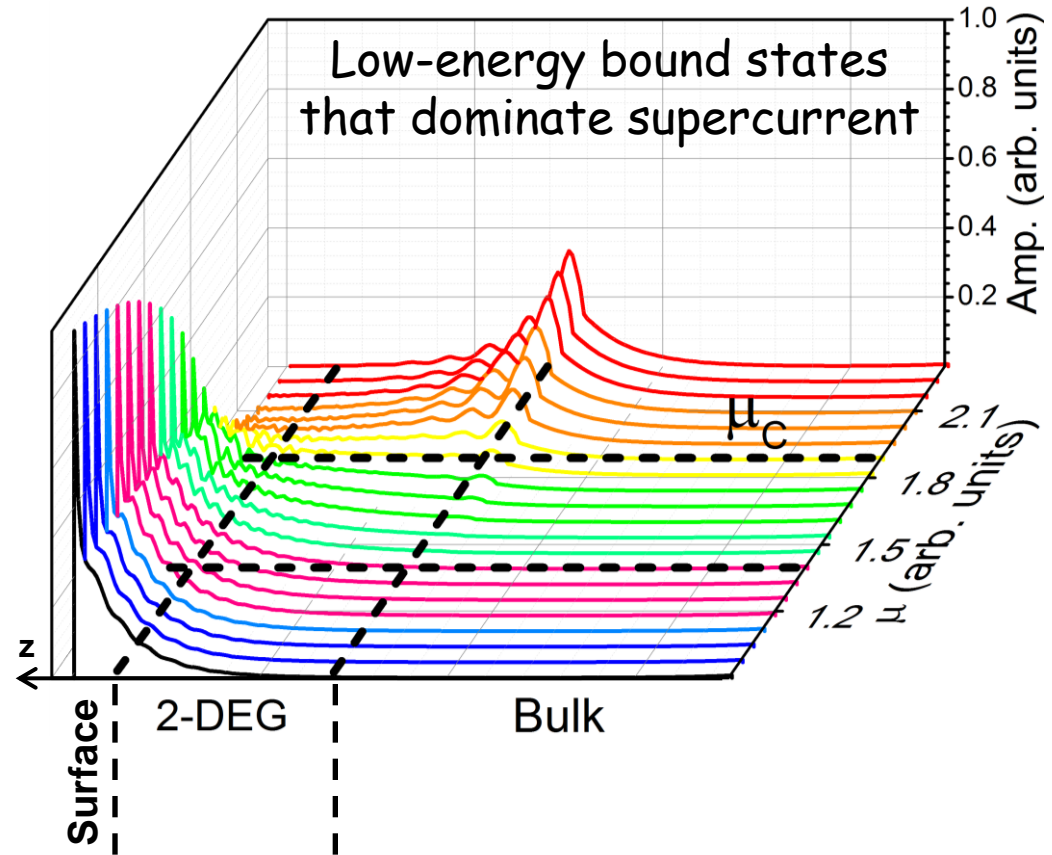


$$\mu < \mu_c$$



Numerical Solutions -- low-energy Andreev Bound States

As μ decreases, the ABS move from the interface between the 2DEG and the insulating region to the free surface \rightarrow topological phase transition

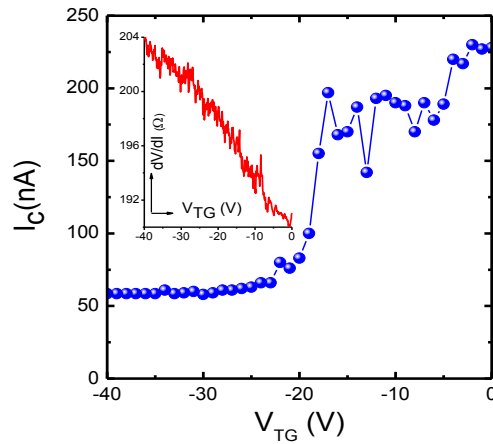


These states carry the majority of the supercurrent which drops because:

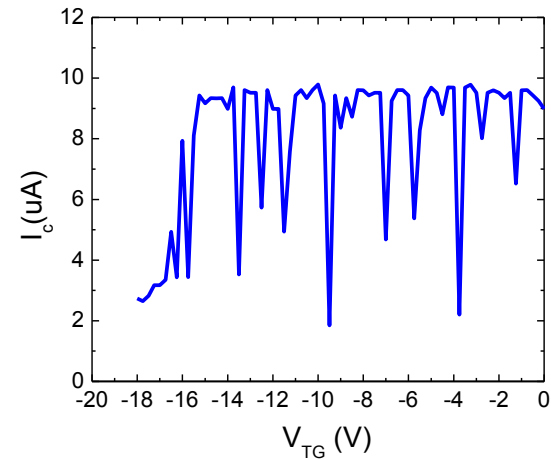
1. The transparency is higher when buried - 2DEG protects the states
2. The transport becomes more diffusive on the surface due to scattering
3. The 2DEG contribution to the supercurrent turns off when depleted

Similar behavior observed in exfoliated crystal devices

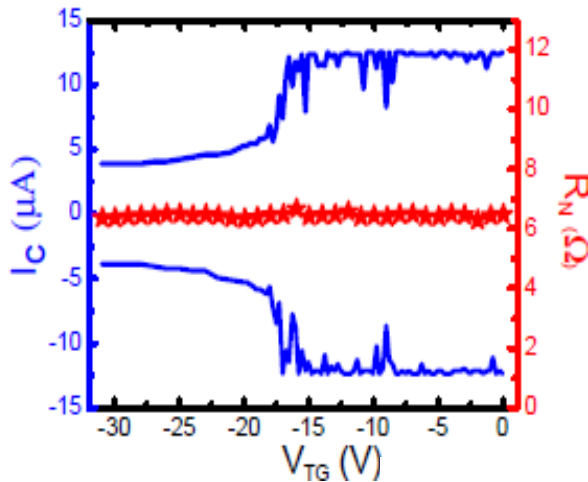
single Josephson junction



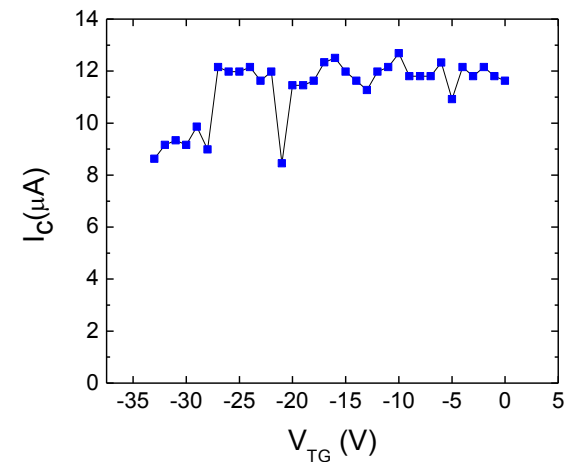
dc SQUID



Trijunction SQUID



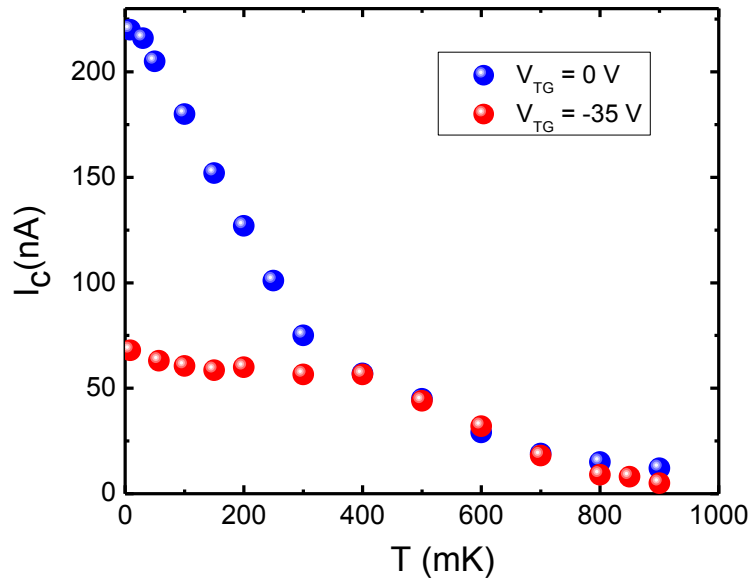
Trijunction SQUID



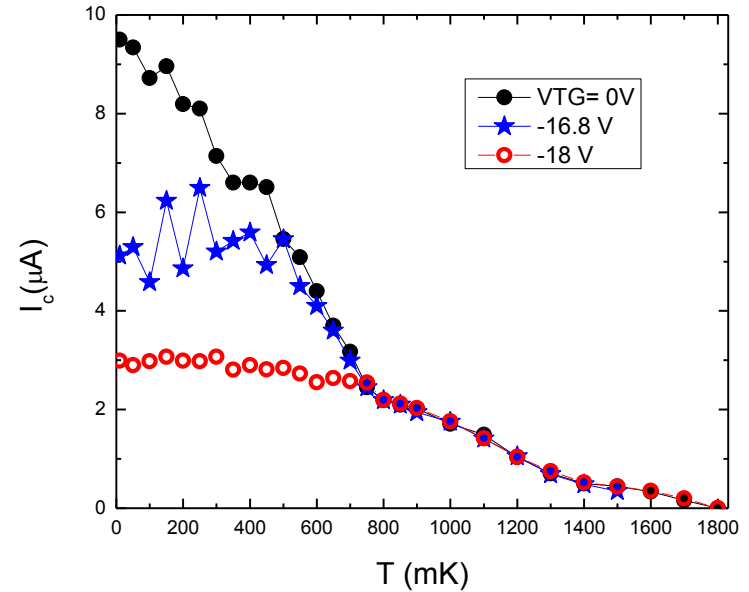
In all case, flat region with large fluctuations followed by a sharp drop

Two-fluid behavior and fluctuations in the temperature dependence

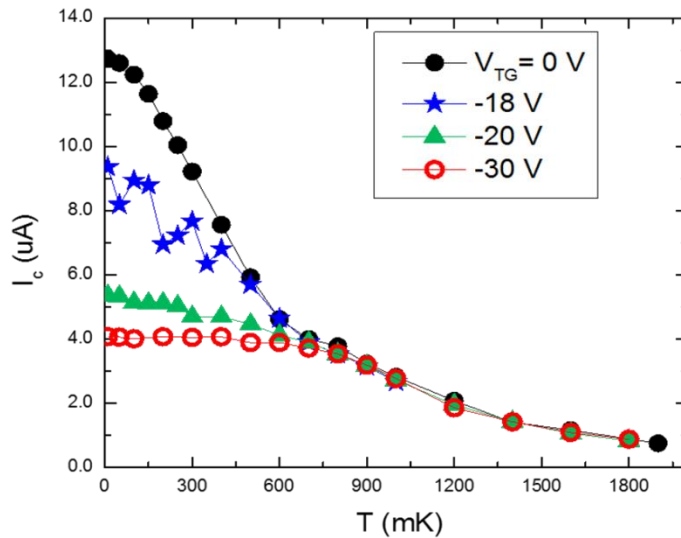
single Josephson junction



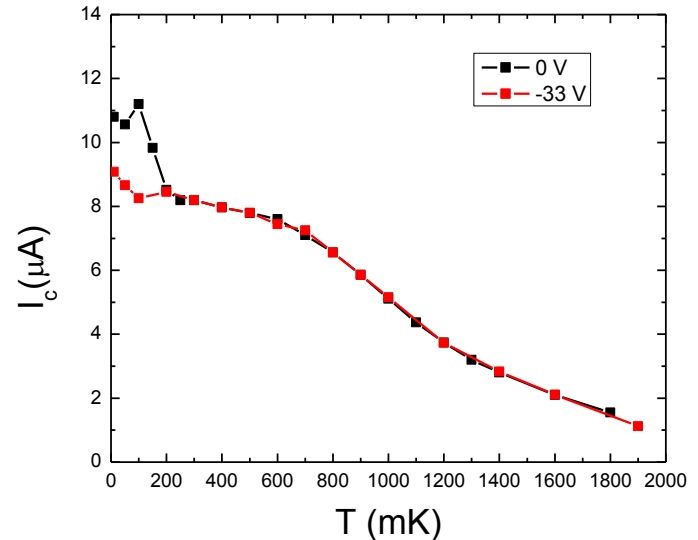
dc SQUID



Trijunction SQUID

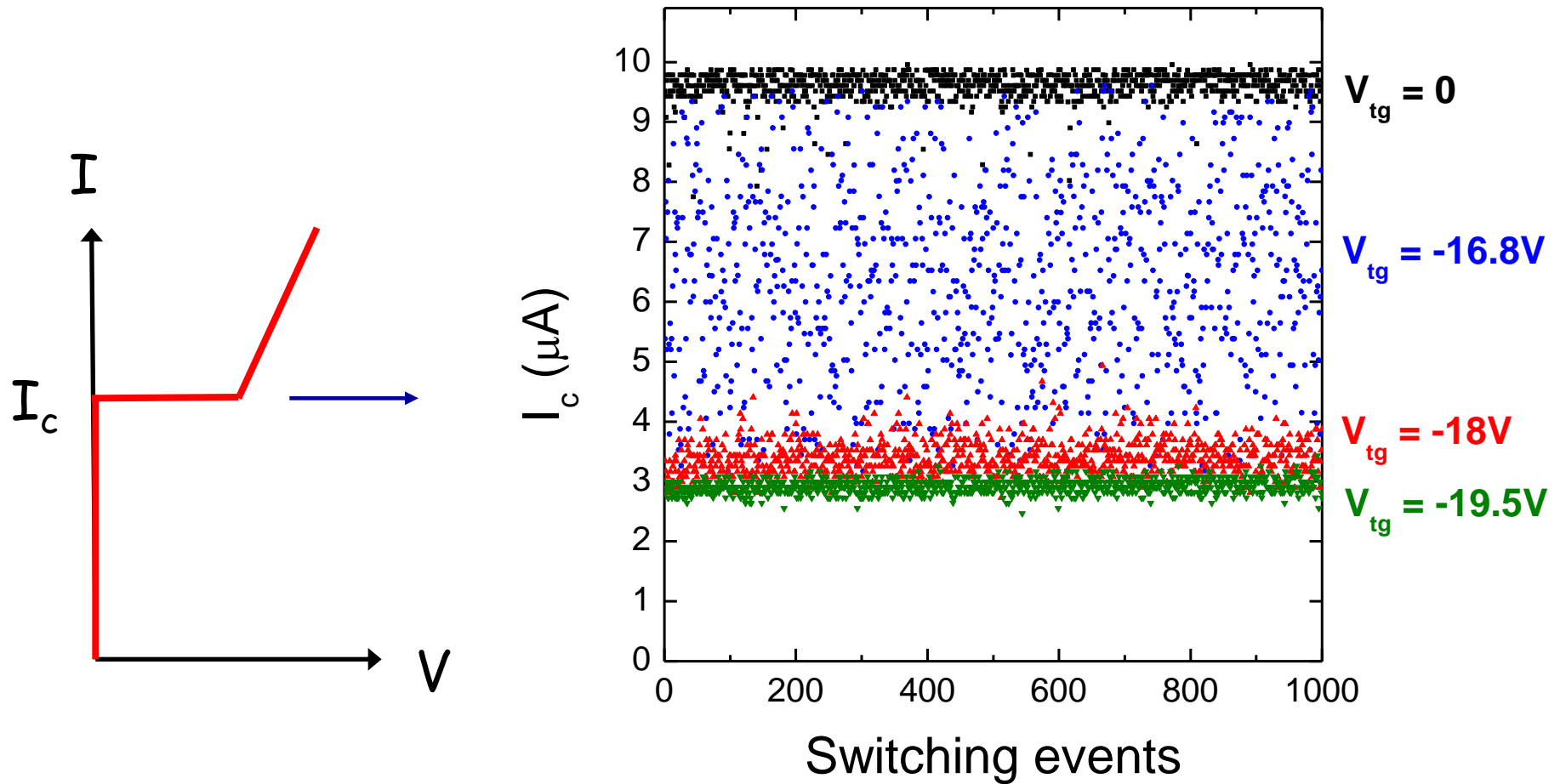


Trijunction SQUID

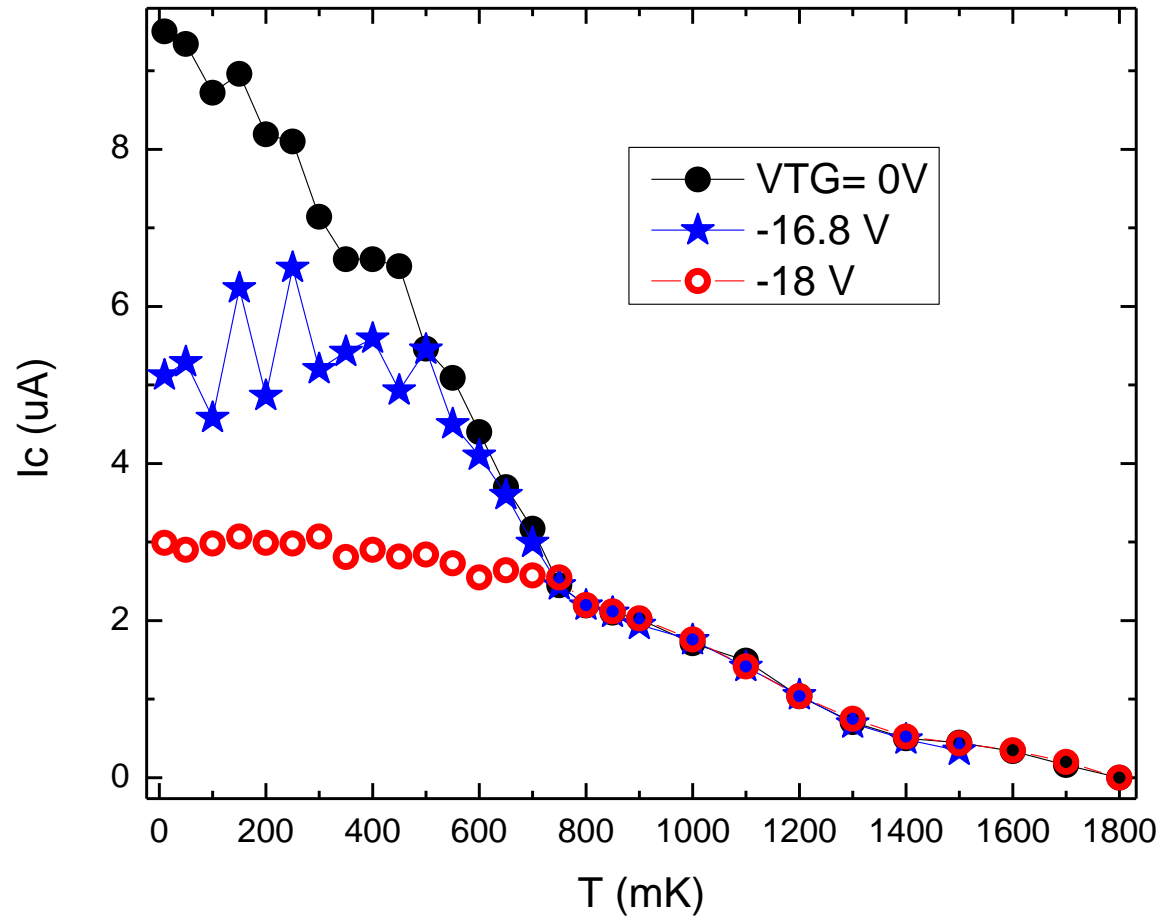
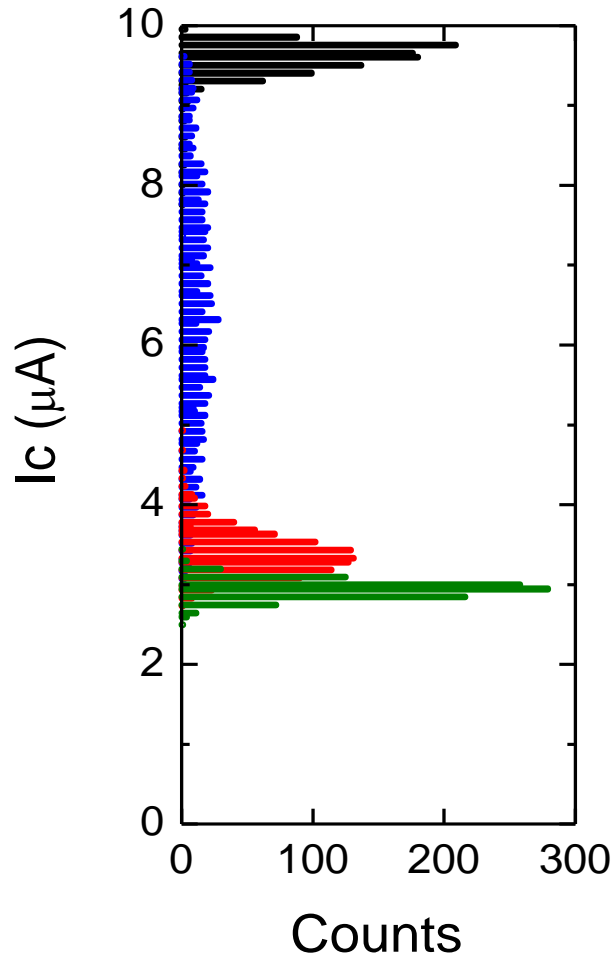


Fluctuations in the critical current

Record 1000 critical current values at each bias by ramping current successively



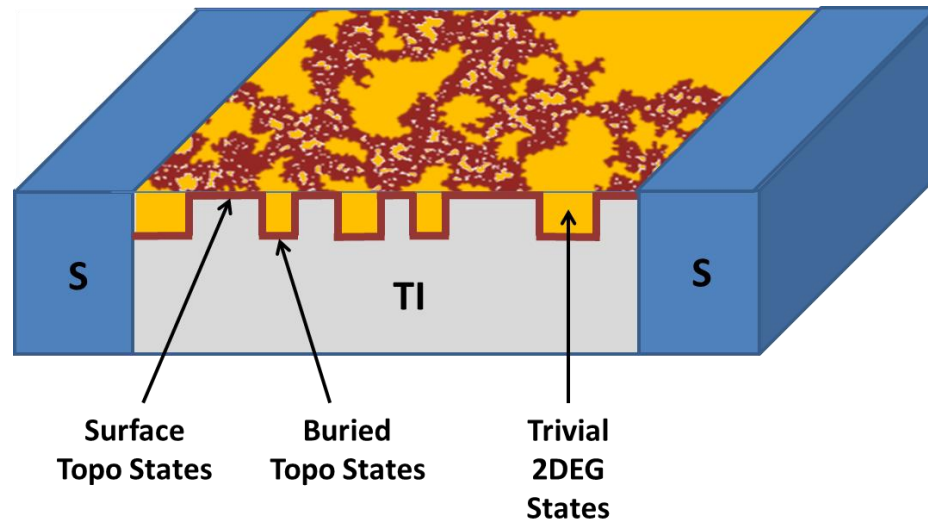
Switching distribution of critical current



Histograms of critical current switches show a broad distribution at intermediate gating --- suggests that the surface state location is fluctuating locally

Physical Picture

Topological surface state winds through 2DEG at intermediate gating



dynamically-meandering topological surface state

Most likely these arise from charge fluctuations in the gate than change the local carrier density and induce the phase transition

Complex system: junction transport will be affected by local switching dynamics, 2D percolation physics, and interactions/avalanches

New microscopic model

Effect of impurities on the Josephson current through helical metals

Pouyan Ghaemi and V. P. Nair

Physics Department, City College of the City University of New York, New York, NY 10031

- Non-magnetic impurity scattering does not affect the conductance (due to spin-momentum locking)
- It does affect the critical current by renormalizing the Fermi velocity, altering the spectrum of the Andreev bound states that carry the supercurrent.
- Condensed matter manifestation of the Mikheyev-Smirnov-Wolfenstein effect, the interaction of matter with neutrinos that lead to flavor oscillations.
- Predicts two-components of the supercurrent --- one affected by impurities, one independent of them --- in agreement with our experiments.